European Journal of Medicinal Chemistry xxx (2018) xxx-xxx

Contents lists available at ScienceDirect

European Journal of Medicinal Chemistry

journal homepage: www.elsevier.com

Research paper

Hydroxyazole scaffold-based *Plasmodium falciparum* dihydroorotate dehydrogenase inhibitors: Synthesis, biological evaluation and X-ray structural studies

Agnese Chiara Pippione[a], Stefano Sainas[a], Parveen Goyal[b, c], Ingela Fritzson[d], Gustavo C. Cassiano[e], Alessandro Giraudo[a], Marta Giorgis[a], Tatyana A. Tavella[e], Renzo Bagnati[f], Barbara Rolando[a], Rhawnie Caing-Carlsson[b], Fabio T.M. Costa[e], Carolina Horta Andrade[g], Salam Al-Karadaghi[h], Donatella Boschi[a], Rosmarie Friemann[b, i], Marco L. Lolli[a, *]

[a] *Department of Science and Drug Technology, University of Turin, via Pietro Giuria 9, 10125, Turin, Italy*
[b] *Department of Chemistry and Molecular Biology, University of Gothenburg, Box 462, S-40530, Gothenburg, Sweden*
[c] *Technologies for the advancement of sciences, Institute for Stem Cell Biology and Regenerative Medicine, Bengaluru, 560065, India*
[d] *Chemoswed, Celsiusgatan 35, 212 14, Malmö, Sweden*
[e] *Laboratory of Tropical Diseases Prof. Luiz Jacintho da Silva, Department of Genetics, Evolution and Bioagents, University of Campinas, 13083-864 Campinas, Brazil*
[f] *Istituto di Ricerche Farmacologiche "Mario Negri" IRCCS, via La Masa 19, 20156, Milan, IT, Italy*
[g] *LabMol, Faculty of Pharmacy, Federal University of Goias, 74605-170, Goiania, Brazil*
[h] *Department of Biochemistry and Structural Biology, Lund University, Sweden*
[i] *Centre for Antibiotic Resistance Research (CARe) at University of Gothenburg, Box 440, S-40530, Gothenburg, Sweden*

ARTICLE INFO

Article history:
Received 2 October 2018
Received in revised form 16 November 2018
Accepted 18 November 2018
Available online xxx

Keywords:
Malaria
Plasmodium falciparum
Dihydroorotate dehydrogenase (DHODH) inhibitors
X-ray-crystallography
Scaffold hopping
Pyrazole
Bioisosterism

ABSTRACT

Plasmodium falciparum dihydroorotate dehydrogenase (*Pf*DHODH) has been clinically validated as a target for antimalarial drug discovery, as a triazolopyrimidine class inhibitor (DSM265) is currently undergoing clinical development. Here, we have identified new hydroxyazole scaffold-based *Pf*DHODH inhibitors belonging to two different chemical series. The first series was designed by a *scaffold hopping* strategy that exploits the use of hydroxylated azoles. Within this series, the hydroxythiadiazole **3** was identified as the best selective *Pf*DHODH inhibitor (IC_{50} 11.0 μM). The second series was designed by modulating four different positions of the hydroxypyrazole scaffold. In particular, hydroxypyrazoles **7e** and **7f** were shown to be active in the low μM range (IC_{50} 2.8 and 5.3 μM, respectively). All three compounds, **3, 7e** and **7f** showed clear selectivity over *human* DHODH (IC_{50} > 200 μM), low cytotoxicity, and retained micromolar activity in *P. falciparum*-infected erythrocytes. The crystallographic structures of *Pf*DHODH in complex with compounds **3** and **7e** proved their binding mode, supplying essential data for future optimization of these scaffolds.

1. Introduction

Malaria is one of the world's "biggest three infectious diseases" (HIV/AIDS, tuberculosis, and malaria) that kill millions of people every year. Effective vaccines have not been developed; thus, chemotherapy remains the mainstay of prevention and treatment. Unfortunately, drug resistance to almost every known antimalarial agent has compromised the effectiveness of control programs: the antimalarial drugs reported so far effectively worked only for certain periods of time until resistance was developed [1]. This justified the search for new approaches for the pharmacological treatment of malaria [2]. One of these approaches was found to be the targeting of *Plasmodium falciparum* dihydroorotate dehydrogenase (*Pf*DHODH), an enzyme involved in the catalysis of the fourth step in *de novo* pyrimidine biosynthesis. [3,4] The *de novo* pyrimidine biosynthesis pathway is crucial to the survival of the parasite: unlike human cells, which are able to utilize the salvage pathway for pyrimidine acquisition, *Plasmodium* species can only access *de novo*-synthesized pyrimidines. Several scaffolds were investigated in the design of new *Pf*DHODH inhibitors (Fig. 1) [3,4]. Among them, the triazolopyrimidine DSM265 was developed by Phillips and co-workers starting from a scaffold discovered in a high-throughput screening [5].

DSM265, a potent inhibitor of the *P. falciparum* and *P. vivax* DHODH with excellent selectivity towards the *P. falciparum* en-

Abbreviations: *pf*DHODH, *Plasmodium falciparum* dihydroorotate dehydrogenase; *h*DHODH, human dihydroorotate dehydrogenase; BOC anhydride, di-*tert*-butyl dicarbonate; NBS, N-bromosuccinimide; TFA, trifluoroacetic acid

* Corresponding author. Department of Science and Drug Technology, University of Turin, via Pietro Giuria 9, 10125, Turin, Italy.
Email address: marco.lolli@unito.it (M.L. Lolli)

https://doi.org/10.1016/j.ejmech.2018.11.044
0223-5234/

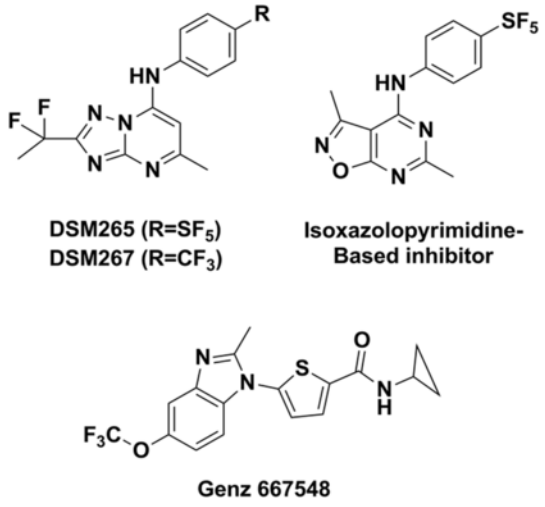

Fig. 1. Structure of DSM265 and other *Pf*DHODH inhibitors.

zyme, as compared to *human* DHODH (*h*DHODH), is the first *Pf*DHODH inhibitor to reach clinical development for the treatment of malaria [5]. Showing both a good safety profile and a long half-life [6], this compound reached phase 2a studies in patients with uncomplicated *P. falciparum* or *P. vivax* malaria infection [7]. During these trials, DSM265 showed single-dose efficacy for the treatment of *P. falciparum* malaria while lower efficacy against *P. vivax*. Unfortunately, recurrent parasites were found in three patients, two of which had mutations in the *dhodh* gene (*dhodh* Cys276Tyr and Cys276Phe respectively). These mutations were shown to be associated with higher EC_{50} values for DSM265 in *in vitro* resistance analysis. This fact emphasizes the need of adding *Pf*DHODH inhibitors with different chemical scaffolds to the human pharmacopoeia. Following this aim, Phillips and co-workers presented recently *Pf*DHODH inhibitors based on an isoxazolopyrimidine scaffold (Fig. 1) [8].

In recent years we have been focusing on targeting *h*DHODH [9–12]. By improving the strategy of scaffold hopping to replace the acidic moieties by acidic hydroxylated azoles in the biologically active lead *brequinar*, we successfully designed a new class of *h*DHODH inhibitors [13–17]. Starting from four acidic hydroxyazoles with a wide range of pK_a values (thiadiazole, pyrazole, triazole and 1,2,5-oxadiazole) [16,18], we first identified compounds with activity in the micromolar range [15,19]. In the following optimization cycle, which involved the 2-hydroxypyrazolo[1,5-a]pyridine scaffold, a lead compound with high on-target activity (sub nanomolar IC_{50}) and low toxicity was identified [20]. In the light of the promising results obtained for the *h*DHODH, and following the same strategy of scaffold hopping, the authors herein applied a similar strategy to design new inhibitors of *Pf*DHODH. Hydroxyazole-4-carboxamides **2**–**6** were initially designed in an attempt to mimic the phenol moiety present in the previously described salicylamide **1** (Fig. 2), [21] an inhibitor that showed low micromolar activity and good selectivity towards the *P. falciparum* enzyme, as compared to *h*DHODH. Compound **1** itself was the result of an extensive SAR study on salicylamides, conducted through the use of various substituents in the salicylic phenyl ring. The study showed the existence of an inverse correlation between the pK_a of the phenolic function and the activity on the enzyme. Compound **1** has the lowest calculated pK_a (6.9) and the highest potency (IC_{50} = 7.0 μM) among tested compounds. Here we will change its benzene scaffold with the aim to improve the acidity of the hydroxyl group and consequently the activity of the resulting compounds. Three acidic hydroxyazoles (hydroxy-1,2,5-oxadiazole, hydroxythiadiazole and hydroxypyrazole), with a range of pK_a values [16,22] near or below 6.9, were included in this first series (Fig. 2).

Of the acidic hydroxyazoles involved, hydroxypyrazole had the weakest acidic profile (pK_a in the range of 6–7), although highly deprotonated at physiological pH. During hit optimization, the two pyrazole ring positions available for substitution provide an opportunity for a better exploration of the chemical space, which allows for accessing additional binding areas of the target protein [23]. For these reasons, and in order to identify new hits besides **1**, a series of pyrazoles that were already present in our library [24,25], were initially assayed for *Pf*DHODH activity. This screening identified **7a** (Fig. 3), as the best *Pf*DHODH inhibitor in the μM range. Pyrazole **7a** is characterized by the presence of a bulky substitution at position 5 and a carboxylic acid function at position 4. With the aim of more extensive study of its SAR, in the following the **7a** structure was extensively investigated by modulating four different positions (Series 2, Fig. 3).

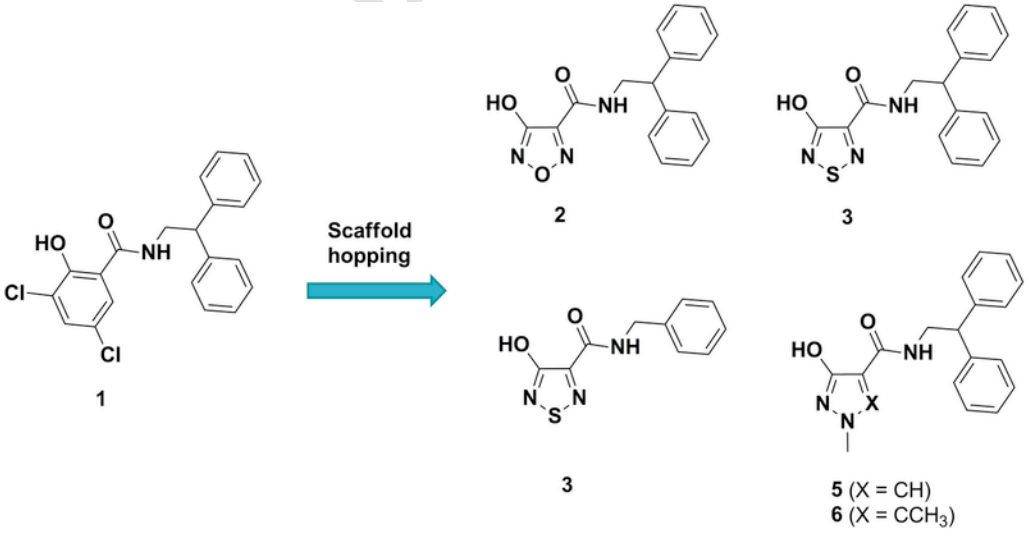

Fig. 2. Structures of compounds **2**–**6** (*series 1*), derived from a scaffold hopping approach to the salicylamide scaffold of **1**.

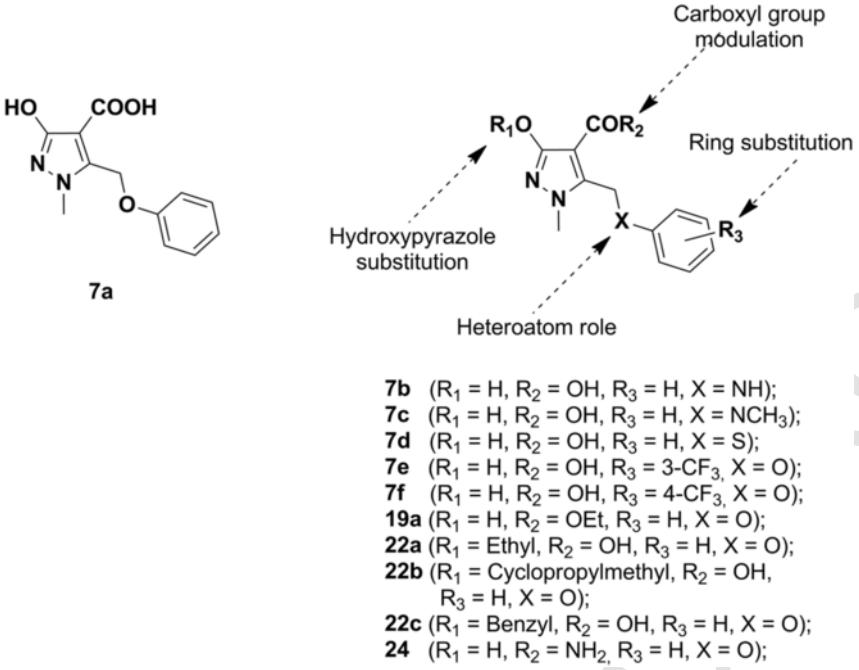

Fig. 3. Modulation of **7a** for the SAR evaluation of *series 2*.

The synthetic strategies used for obtaining the two designed series of compounds are presented here and fully discussed together with the compounds' biological profile in enzymatic and cell-based assays. The X-ray crystallography structures of the ligand - *Pf*DHODH complexes of the most representative compounds were also determined in order to identify experimentally the binding poses.

2. Result and discussion

2.1. Chemistry

The synthetic methodologies for the preparation of compounds **2**–**6** (series 1) are shown in Scheme 1. To obtain the 1,2,5-oxadiazole derivative **2,** the benzyloxy moiety was removed from the known methyl ester **8** [26] by catalytic hydrogenation and the obtained crude methyl 4-hydroxyfurazancarboxylic ester was directly treated with the 2,2-diphenylethanamine at 60 °C. A similar strategy was used also for the synthesis of thiadiazole amides **3** and **4**. The nitrile group in the known intermediate **9** was therefore transformed into the corresponding methyl ester **10** by a Pinner reaction. The ester was then allowed to react with the specific amines, which act both as reagents and solvents, at 60 °C, in order to generate the desired amides **3** and **4**. The amides **5** and **6** were obtained from known acids **11** [27] and **12** [15] by coupling with 2,2-diphenylethanamine and reducing by catalytic hydrogenation the obtained benzyl-protected amides **13** and **14**.

Scheme 2 describes the strategies used in the synthesis of the 3-hydroxy-N(1)methyl-1H-pyrazole-4-carboxylic acid analogues **7a-f** of the series 2. The hydroxy group in position 3 of the known compound **15** [15] was protected via treatment with BOC anhydride giving **16**. The bromination of methyl substituent in **16** was performed using N-bromosuccinimide (NBS) and benzoyl peroxide, as the catalyst agent, giving compound **17** (48% yield), which is the key intermediate in the production of the following series. In fact, the corresponding alkylated analogues (**18a-f**), were obtained via the reaction of **17** with a variety of nucleophiles. The hydroxy group on **18a-f** was subsequently restored via treatment with trifluoroacetic acid (TFA), yielding the series **19a-f**. In the following step, the ester functions present in **19a-f** were finally hydrolysed giving the corresponding acids **7a-f**.

The synthetic strategies used to obtain the O-alkylated pyrazoles **22a-c** and the amide **24** are shown in Scheme 3. Since the 3-hydroxypyrazole **19a** can present two tautomeric forms (Scheme 3) [28], both O— and N— alkylation patterns must be taken into account when considering its reactivity. The alkylation pattern in similar hydroxyazole systems is usually governed by the choice of the alkylating agent and the heteroatoms present in the heteroazole system [29]. The treatment of **19a** with three different alkylating agents produced compounds **21a-c,** as the only reaction products in each case. The three compounds, characterized using diagnostic ^{1}H— ^{13}C NMR chemical shifts, were identified as O-alkyl isomers. The methylene chemical shifts of the added substituents appear in ^{1}H NMR spectra above 4 ppm (**21a** δ = 4.29 ppm; **21b** δ = 4.07 ppm; **21c** δ = 5.32 ppm), while in ^{13}C NMR spectra between 65 and 71 ppm (**21a** δ = 64.9 ppm; **21b** δ = 73.6 ppm; **21c** δ = 70.3 ppm) (Fig. 4). This behaviour is incompatible with the upfield N-alkylation pattern found in known N-substituted hydroxypyrazoles, such as 1,2-diethylpyrazolidine-3,5-dione **20a** [30], (Fig. 4) but is in accordance with the downfield O-alkylation pattern found in known O-substituted hydroxyazoles, such as 3-hydroxytriazole **20b** [31] (Fig. 4).

In the following step, the ester moieties present in **21a-c** were hydrolysed in aqueous NaOH giving the corresponding acids **22a-c**. Acid **22c** was transformed into the corresponded acyl chloride which reacted with aqueous ammonia in THF to produce protected amide **23**. The benzyl moiety of **23** was then removed using catalytic hydrogenation at atmospheric pressure, giving the desired amide **24**.

2.2. Inhibition of PfDHODH and structure-activity relationships (SAR)

The inhibitory activity of the compounds **2**–**6**, **7a-f**, **19a**, **22a-c** and **24** was initially evaluated on recombinant *Pf*DHODH assay

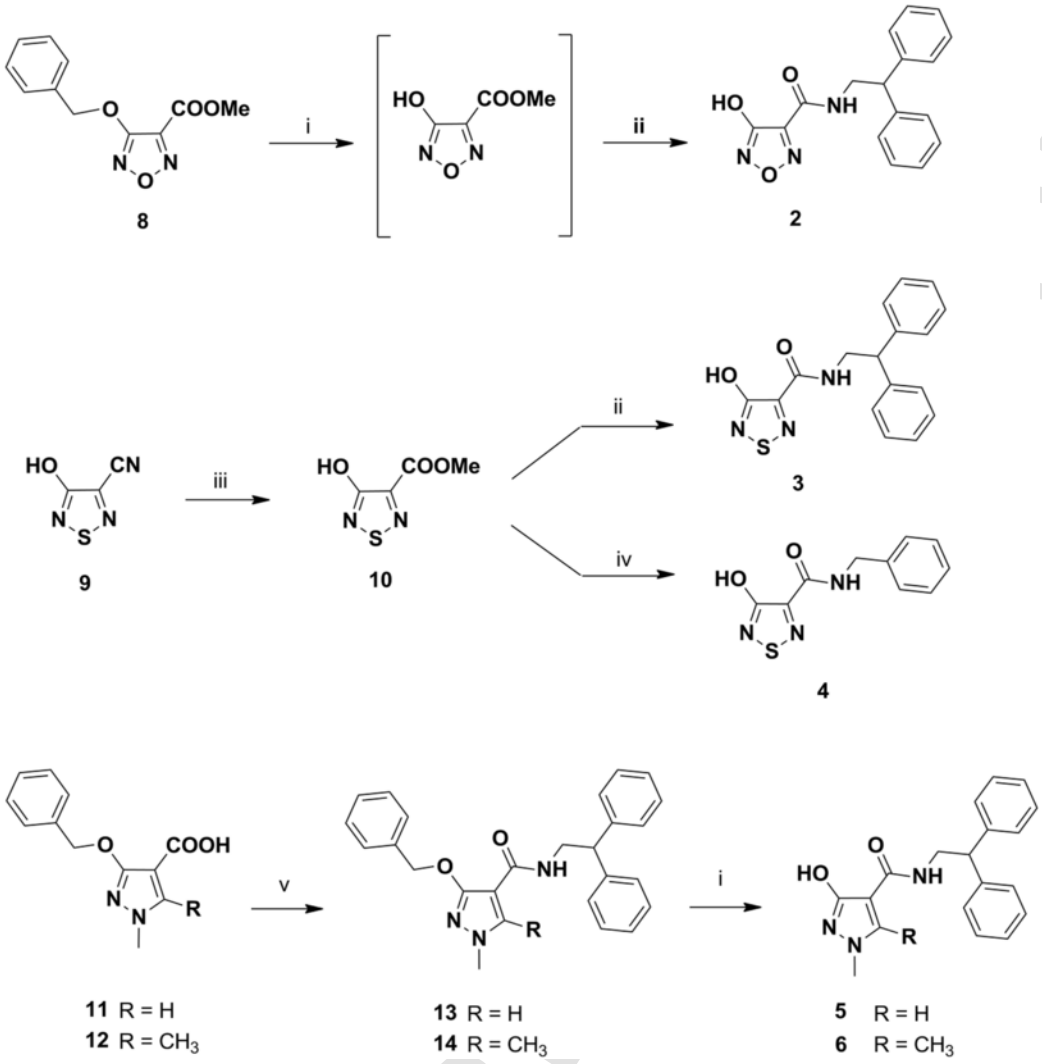

Scheme 1. Reagents and conditions: i) H_2, Pd/C, dry THF; ii) 2,2-diphenylethanamine, 60 °C; iii) a) NaH, MeOH; b) 2M H_2SO_4; iv) benzylamine, 60 °C. v) HBTU, 4-(dimethylamino)pyridine (DMAP), 2,2-diphenylethanamine, dry DMF.

(Table 1). An analysis of the compounds in series 1 showed how compounds **2**–**4** present an interesting micro-molar activity while compounds **5** and **6** were totally inactive. Compound **3** is the most active, although it was not able to give better results than compound **1** in either *Pf*DHODH or *h*DHODH/*Pf*DHODH ratio. These data indicates that the hydroxy-1,2,5-oxadiazole moiety present in compound **2**, and the hydroxythiadiazole moiety present in **3** and **4**, are both able to successfully mimic the phenolic moiety present in **1.** Hydroxypyrazole instead, present in compounds **5** and **6,** was not able to efficiently modulate the same portion of compound **1**.

In series 2 (**7a-f**, **19a**, **22a-c**, **24**) the presence of broader chemodiversity allows a more extensive SAR evaluation. Thus, the presence of the 3-hydroxy and 4-carboxy functions on the pyrazole ring is essential for activity as shown by **7a** (IC_{50} = 19 μM). Every alkylation of the 3-hydroxy group of **7a** (compounds **22a-c**) resulted in the absence of activity. Also compounds **19a** and **24**, bearing 4-ethyl carboxylate and 4-amidic function, respectively, are inactive. Successively, maintaining the 3-hydroxy and 4-carboxy functions, the 5-substitution of the pyrazole ring was investigated in compounds **7b-f**. The replacement of the ethereal oxygen of **7a** with its isosters NH (**7b,c**), and sulphur (**7d**), was well accepted by the target, although no relevant activity benefit could be observed. However, trifluoromethyl substitution in the 3 and 4 positions of the phenoxy group moved the IC_{50} to the low μM range making **7e** and **7f** the most active and interesting compounds in the series. In order to check for selectivity, the compounds that show activity against *Pf*DHODH (**2**, **3**, **4**, **7a-f**), were also assayed for activity on recombinant *h*DHODH (Table 1). Both series have IC_{50} > 200 μM on *h*DHODH, thus proving high selectivity towards *Pf*DHODH. In particular, compound **7e** showed the highest *h*DHODH/*Pf*DHODH activity ratio (ratio >71).

*2.3. Binding mode analysis of PfDHODH co-crystallized in complex with compounds **3** and **7e***

Structure determination of *Pf*DHODH in complex with a range of chemo-diverse inhibitors has recently offered valuable insights into the structural basis of inhibition of the enzyme (see Pavadai et al. [33] and references within). In order to experimentally evaluate the binding modes of the various compounds in this paper and to support SAR studies, the crystal structures of *Pf*DHODH in complex with the two series' most significant inhibitors, thiadiazole **3** and hydroxypyrazole **7e**, have been determined. The structures were determined using

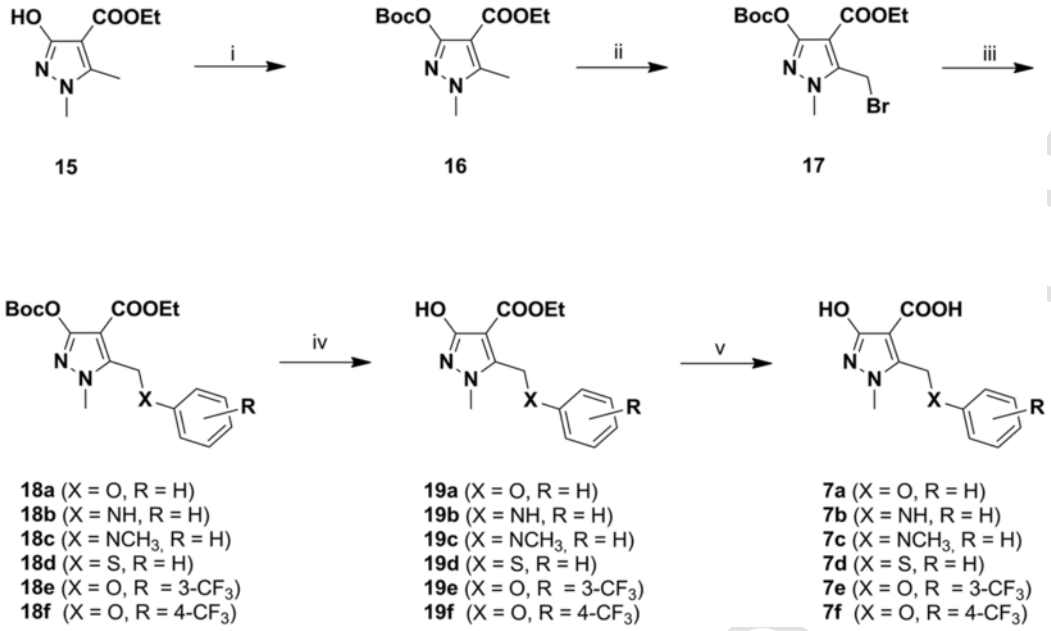

Scheme 2. Reagents and conditions: i) Cs_2CO_3, BOC anhydride, dry THF, reflux; ii) NBS, benzoyl peroxide, dichloroethane, reflux; iii) R-(Ph)-XH, Cs_2CO_3, dry DMF; iv) TFA, DCM; v) 5M NaOH, EtOH; vi) R_1X, K_2CO_3, acetonitrile; vii) a) oxalyl chloride, dry DMF, dry THF, 0 °C; b) aq NH_3, THF; viii) H_2, Pd/C, dry THF.

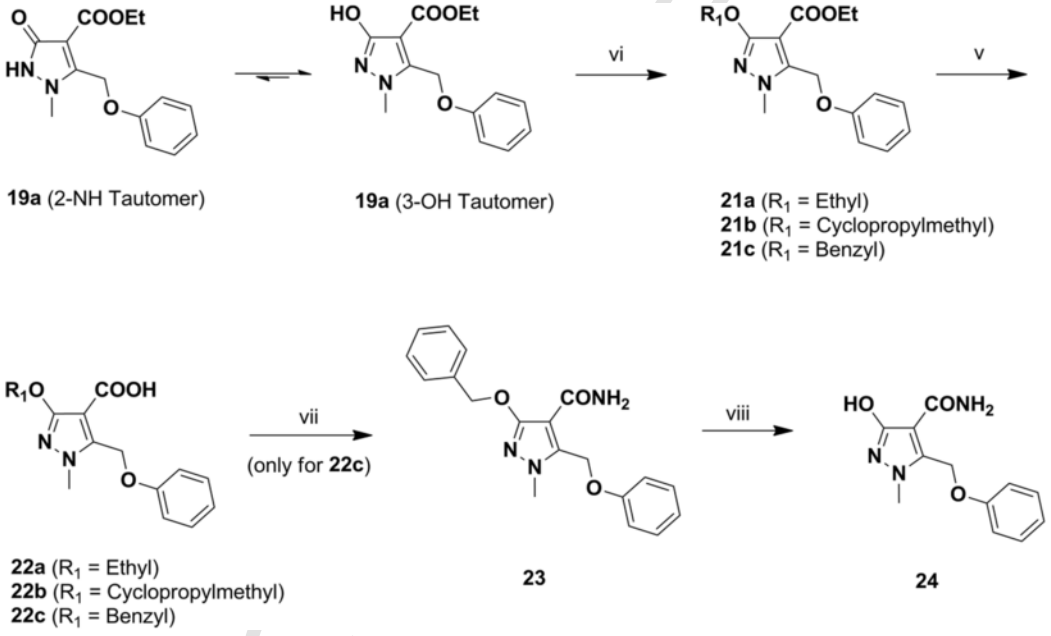

Scheme 3. Reagents and conditions: vi) R1X, K2CO3, acetonitrile; vii) a) oxalyl chloride, dry DMF, dry THF, 0 °C; b) aq NH3, THF; viii) H2, Pd/C, dry THF.

molecular replacement and were refined to 1.95 Å (**3**, PDB id: 6I55), and 1.98 Å resolution (**7e,** PDB id: 6I4B), with good stereochemistry. X-ray data collection and refinement statistics are summarised in Table S2. The three-dimensional fold of *Pf*DHODH in the inhibitor bound complexes is similar to previously reported structures of *Pf*DHODH in complex with A77-1726, and with other triazolopyrimidine-related compounds (Deng et al. [34] and references within). Deng et al. [34] have elucidated the structural basis of the species-selective binding of triazolopyrimidines to *Pf*DHODH, and identified the key amino acid residues that confer selectivity. A comparison of *h*DHODH and *Pf*DHODH crystal structures revealed that the replacement of Ala59 and Pro364 residues in *h*DHODH by the bulkier Phe188 and Met536, which are found in *Pf*DHODH, makes inaccessible the hydrophobic pocket that binds the biphenyl moiety of brequinar in *h*DHODH [34]. A comparison of *Pf*DHODH structure in complex with compounds **3** and **7e** (Fig. 5), shows that both compounds are able to occupy the lipophilic pocket formed by Phe171, Leu172, Leu187, Phe188 and Met536 using a phenyl in **3** and the 3-(trifluoromethyl)phenyl moiety in **7e**. Noteworthy, the biggest differences in the *human* and *P. falciparum* DHODH enzymes are found in the same hydrophobic pocket, meaning that this region is crucial for

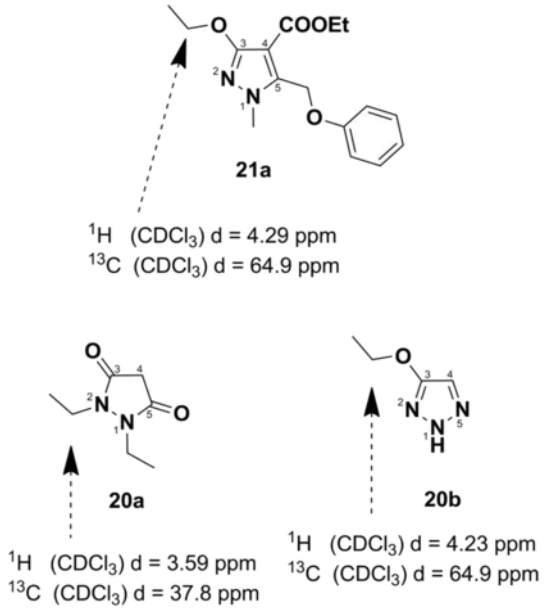

Fig. 4. Comparison of NMR chemical shifts for compounds **21a, 20a** and **20b**.

selectivity [35] (the *Pf*DHODH-**7e** complex with the non-conserved residues of the binding site highlighted is depicted in Fig. S1).

The different roles played by the hydroxyazole moieties in compounds **3** and **7e** are quite interesting. In order to better understand the role of the acidic moiety, the pK_a values of compounds **2**–**6** were determined (Table S1). The hydroxy group in **3** (Fig. 5A), which is deprotonated at physiological pH (misured pK_a = 3.72, Table S1), is pointing toward His185 and makes a key polar interaction. Hydroxy-1,2,5-oxadiazole **2** has the lowest pK_a value (3.33), followed by thiadiazole derivative **4** (3.69), and the hydroxypyrazole derivatives **5** and **6** (pK_a of 6.42 and 6.54, respectively; see Table S1), these latter being the weakest acids. This polar interaction is presumed to be lost in pyrazoles **5** and **6** for their higher pK_a values. The sulphur present in the **3** thiadiazole ring was found to be pointing toward a relatively lipophilic area, associated with Ile272 and Ile263, where it is able to form interactions. The polar feature of 1,2,5-oxadiazole oxygen in **2** is unable to play such a role, meaning that the affinity of **2** is lower. Although pyrazoles **5** and **6** are probably able to project a methyl group in the right direction, however, due to their reduced acidity the interaction with His185 should be much weaker. In **3**, the carbonyl of the amide moiety appears to interact effectively with the side chain of Arg265, being at a distance of 2.75 Å.

Binding of the hydroxypyrazole compound **7e** (Fig. 5B) shows how the free carboxylate is necessary for the interaction with His185. The deprotonation of this group under physiological conditions supports the hypothesis obtained from SAR studies, that neutral carboxylate analogues (**19a** and **24**) are inactive. A comparison of **7e** with **3** shows that the presence of the carboxylate totally changes the orientation of the hydroxy group in the active site. Compound **7e** establishes an interaction with Arg265 side chain via its N(2) nitrogen, while its hydroxy group is pointing toward the sub-pocket, associated with Ile272 and Ile263. The alkylation/benzylation of the hydroxyl group resulted in an absence of activity of compounds **22a-c**, meaning that ethyl, cyclopropylmethyl and benzyl substituents are probably too bulky to fit the abovementioned sub-pocket (Ile272 and Ile263).

2.4. Growth inhibition assays in P. falciparum-infected erythrocytes and mammalian cells

The three most potent compounds against *Pf*DHODH (**3**, **7e** and **7f**), were assayed in whole cell *P. falciparum* 3D7 (cloroquine-sensitive strains). The results are summarized in Table 1. Moreover, the three compounds were also assayed in fibroblast-like cell lines derived from monkey kidney tissue (COS-7 cells), to test their cytotoxicity in mammalian cells (Table 1). Importantly, the cytotoxicity val-

Table 1
Biological activity of synthesized compounds on isolated DHODHs and cells.

	Compound	*Pf*DHODH[a] IC_{50} ± SE (μM)	*h*DHODH[b] IC_{50} ± SE (μM)	Ratio IC_{50} value (*h*- vs *Pf*-ratio)	*P. falciparum* 3D7 cells[c] EC_{50} ± SE (μM)	COS-7 cells[d] CC_{50} μM (CI 95%)[e]
	DSM1	0.065	n.d.	n.d.	n.d.	n.d.
	1	7.0[f]	>200[f]	>29	n.d.	n.d.
Serie 1	**2**	75 ± 19	>200	>3	n.d.	n.d.
	3	12 ± 1	>200	>17	35.9 ± 5.96	189.9 (181.0–199.2)
	4	35 ± 1	>200	>6	n.d.	n.d.
	5	>250	n.d.	n.d.	n.d.	n.d.
	6	>250	n.d.	n.d.	n.d.	n.d.
Serie 2	**7a**	19 ± 1	>250	>13	n.d.	n.d.
	7b	16 ± 1	>250	>16	n.d.	n.d.
	7c	23 ± 1	>250	>10	n.d.	n.d.
	7d	25 ± 3	>250	>10	n.d.	n.d.
	7e	2.8 ± 0.3	≥200	>71	40.7 ± 9.58	166.7 (133.9–207.5)
	7f	5.3 ± 1.2	≥200	>38	26.7 ± 7.09	152.1 (137.0–168.8)
	19a	>250	n.d.	n.d.	n.d.	n.d.
	22a	>250	n.d.	n.d.	n.d.	n.d.
	22b	>250	n.d.	n.d.	n.d.	n.d.
	22c	>250	n.d.	n.d.	n.d.	n.d.
	24	>250	n.d.	n.d.	n.d.	n.d.

Effect of the compounds on.

[a] *P. falciparum* DHODH (*Pf*DHODH) recombinant enzyme; DSM-1 was used as a reference compound; the measured IC_{50} is comparable to a previously-reported IC_{50} value, [32].

[b] *h*DHODH recombinant enzyme.

[c] growth inhibition assay on *Plasmodium falciparum* 3D7 (cloroquine-sensitive strain).

[d] cytotoxicity assay on fibroblast-like cell lines derived from monkey kidney tissue (COS-7 cells).

[e] error represents the 95% confidence interval of the fit.

[f] data previously reported [21]. The "n.d." notation indicates that the compound was not tested in that specific assay.

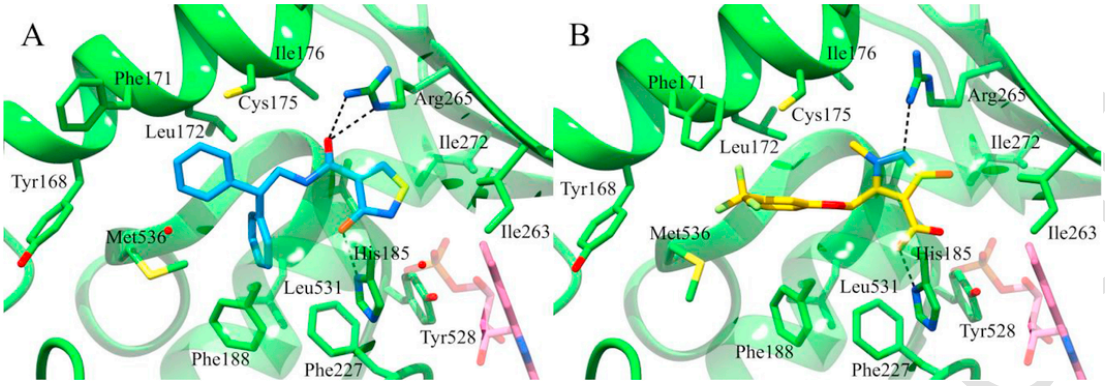

Fig. 5. Structure of *Pf*DHODH co-crystallised with compound **3** (Fig. 5A, PDB id: 6I55) and **7e** (Fig. 5B, PDB id: 6I4B). Nitrogen, fluorine, oxygen and sulphur atoms are depicted in blue, green, red and yellow, respectively. H-Bond are represented by dash line. The figure was produced using the UCSF Chimera package [36]. (For interpretation of the references to colour in this figure legend, the reader is referred to the Web version of this article.)

ues for mammalian cells were very low (CC_{50} > 100 μM), which is in agreement with the compounds' inactivity in *h*DHODH (Table 1). It can therefore be stated that the compounds were highly selective against the parasite, although they did not exhibit the low micromolar activity that will inevitably be required for new antimalarial candidate compounds. The anti-plasmodial activity data for these new derivatives is interesting for the novelty of their scaffolds.

3. Conclusions

We herein describe the synthesis of two series of new *Pf*DHODH inhibitors based on the hydroxyazole scaffold. In the first series of compounds, the 2-hydroxy-3,5-dichlorophenyl moiety of **1** [21], was replaced with three different hydroxyazole systems (**3** as best compound). The second series includes a modulation of a 3-hydroxypyrazol-4-carboxylic acid, a scaffold that had never before been explored in the field of *Pf*DHODH inhibition. This led to the identification of **7e**, which selectively inhibited *Pf*DHODH *in vitro* and achieved a single digit μM IC_{50} value. **7e** was also active on the parasite (40.7 μM). The crystal structures of the complexes between the most interesting compounds in the two series (compounds **3** and **7e**), and *Pf*DHODH led to the identification of their binding modes, which is essential for the subsequent application of a *hit-to-lead* process necessary to improve their activity and drug-like properties. These studies are under development and will be the subjects of forthcoming publications.

4. Experimental section

4.1. Chemistry

General methods. All chemical reagents were obtained from commercial sources (Sigma Aldrich, Alfa Aesar), and used without further purification. Thin-layer chromatography (TLC), was performed to monitor the reaction processes. Analytical grade solvents (acetonitrile, diisopropyl ether, diethyl ether, dichloromethane [DCM], dimethylformamide [DMF], ethanol 99.8% v/v, ethyl acetate, methanol [MeOH], petroleum ether b.p. 40–60 °C [petroleum ether]), were used without further purification. When required, solvents were dried on 4 Å molecular sieves. Tetrahydrofuran (THF), was distilled from Na and benzophenone under N_2 immediately prior to use. Thin layer chromatography (TLC), was carried out on silica gel on 5 × 20 cm plates with a 0.25 mm layer thickness. Anhydrous $MgSO_4$ was used as a drying agent for the organic phases. Compound purification was achieved using flash column chromatography on silica gel (Merck Kieselgel 60, 230–400 mesh ASTM), and the eluents indicated by CombiFlash Rf 200 (Teledyne Isco), at 5–200 mL/min, 200 psi (with automatic injection valve), in RediSep Rf Silica columns (Teledyne Isco) with the eluents indicated below. Compounds synthesized in our laboratory generally varied between 90% and 99% purity. Biological experiments were carried out on compounds with a purity of at least 95%. Purity was checked using two analytical methods. HPLC analyses were performed on a UHPLC chromatographic system (Perkin Elmer, Flexar). The analytical column was a UHPLC Acquity CSH Fluoro-Phenyl system (2.1 × 100 mm, 1.7 μm particle size) (Waters). Compounds were dissolved in either acetonitrile or MeOH and injected through a 20 μL loop. The mobile phase consisted of acetonitrile/water with 0.1% trifluoroacetic acid; two mobile phase gradient profiles were used to assay the purity of each compound. UHPLC retention times were obtained at flow rates of 0.5 mL/min and the column effluent was monitored at 215 and 254 nm, referenced against a 360 nm wavelength. Melting points (m.p.), were measured on a capillary apparatus (Büchi 540). Final m.p. determination was achieved by placing the sample at a temperature that was 10 °C below the m.p. and applying a heating rate of 1 °C min^{-1}. All compounds were routinely checked using ^1H and ^{13}C NMR and mass spectrometry. The IR spectra of the target compounds (**2–6**, **19a**, **7a - f**, **22a – c** and **24**), were recorded on FT-IR (PerkinElmer SPECTRUM BXII, KBr dispersions), using diffuse reflectance apparatus DRIFT ACCY. MS spectra were performed on a Finnigan-Mat TSQ-700 system (70 eV, direct inlet for chemical ionization [CI]), while ^1H and ^{13}C NMR spectra were performed on a Bruker Avance 300 instrument. The following abbreviations are used for coupling patterns: br = broad, s = singlet, d = doublet, dd = doublet of doublets, t = triplet, q = quartet, m = multiplet. Chemical shifts (*δ*), are given in parts per million (ppm). The HRMS spectra of the final compounds (**2–6**, **19a**, **19e**, **19f**, **7a – 7f**, **22a - 22c** and **24**), were recorded on a LTQ Orbitrap XL plus (Thermo Fisher Scientific, Waltham, MA USA), equipped with an ESI ionization source, with positive or negative ions (Spray capillary voltage: 3000 V (+), 2500 V (−)). Compounds **7** [26], **9** [37], **11** [27], **12** [15] and **15** [15] were prepared according to procedures that have already been described.

4.1.1. N-(2,2-diphenylethyl)-4-hydroxy-1,2,5-oxadiazole-3-carboxamide (2)

Pd/C (0.050 g), was added to a solution of methyl 4-(benzyloxy)-1,2,5-oxadiazole-3-carboxylate (compound 8 [26], 200 mg, 0.854 mmol), in dry THF and the suspension was stirred at room temperature under a hydrogen atmosphere for 2 h. The reaction mixture

was filtered off through a short layer of celite and the layer was washed with methanol. The solvent was evaporated, taken with methanol and re-evaporated under reduced pressure (this step was repeated three times). The residue was directly used in the next step; it was mixed with 337 mg (1.71 mmol), of 2,2-diphenylethan-1-amine and the mixture was heated at 60 °C until the melting of the amine occurred. The mixture was stirred and heated at 60 °C overnight, then cooled to room temperature and diluted with 15 mL of 1N NaOH. The aqueous solution was washed twice with diethyl ether, then acidified with 3N HCl to pH 2 and extracted with DCM (3 × 25 mL). The organic layers were collected, dried over anhydrous Na2SO4 and concentrated under reduced pressure to afford 2 as a white solid (m.p. 136.6–137.1 °C; with diisopropylethyl ether). Yield 61%; 1H NMR (300 MHz, DMSO-d_6, ppm), δ 3.92 (dd, 2H, J = 7.7 Hz, J = 5.9 Hz, —CH2CH(Ph)2); 4.36 (t, J = 7.9 Hz, 1H, —CH2CH(Ph)2); 7.37–7.14 (m, 10H, aromatic protons), 8.75 (t, J = 5.3 Hz, 1H, —CH2NHCO—). Exchangeable proton signals overlapped with the water signal. 13C NMR (75 MHz, DMSO-d_6, ppm), δ 43.2, 49.6, 126.3, 127.8, 128.4, 142.3, 142.6, 156.2, 161.8. MS (CI): m/z = 310 [M+H]+. IR (KBr, cm-1), ν: 3399.1, 3026.4, 1684.0, 1607.8, 1560.0, 1272.4, 1199.7, 706.2. EI-HRMS (M + H)+ found 310.1188, calculated for C17H16N3O3 310,1186.

*4.1.2. Methyl 4-hydroxy-1,2,5-thiadiazole-3-carboxylate (**10**)*

A 60% dispersion of sodium hydride in mineral oil (315 mg), was added to a solution of 9 (500 mg, 3.93 mmol), in dry methanol (30 mL). The reaction mixture was stirred under a nitrogen atmosphere at 0 °C for 15 min, then allowed to reach room temperature and further stirred for 60 min 2M H2SO4 (10 mL), was slowly added and the reaction mixture was cooled to 0 °C. The resulting suspension was extracted twice with DCM. The organic layers were collected, dried and concentrated under reduced pressure. The crude material was purified by flash chromatography using DCM/MeOH 90:10 v/v as the eluent to afford the title compound as a white solid (m.p. 90.6–91.2 °C). Yield 55%. 1H NMR (300 MHz, DMSO-d_6, ppm), δ 3.86 (s, 3H, —CH3O-), 13.13 (br s; 1H; —OH). 13C NMR (75 MHz, DMSO-d_6, ppm), δ 52.3, 138.1, 159.3, 164.8; MS (CI): m/z = 161 [M+H]+. IR (KBr, cm-1), ν: 3306.0, 1690.0, 1526.9, 1379.4, 1130.2, 945.0, 684.9.

*4.1.3. N-(2,2-diphenylethyl)-4-hydroxy-1,2,5-thiadiazole-3-carboxamide (**3**)*

10 (100 mg, 0.624 mmol), was mixed with 2,2-diphenylethanamine (246.4 mg, 1.249 mmol), and the mixture was heated at 60 °C (melting of start material), overnight. The mixture was cooled to room temperature and diluted with 2N HCl (10 mL). The solution was extracted using DCM (4 × 15 mL), the organic layers were collected, dried over anhydrous Na_2SO_4 and concentrated under reduced pressure to afford **3** as a white solid (m.p. 117.6–118.0 °C with isopropanol). Yield 83%; ^{1}H NMR (300 MHz, $CDCl_3$, ppm), δ 4.10 (dd, J = 7.7, 6.3 Hz, 2H; —CH_2CH(Ph)$_2$), 4.30 (t, J = 7.9 Hz, 1H, —CH$_2$CH(Ph)$_2$), 6.96 (br s; 1H—CH$_2$NHCO—), 7.21–7.40 (m; 10H, *aromatic protons*), 10.87 (br s; 1H, —OH). ^{13}C NMR (75 MHz, $CDCl_3$, ppm), δ 43.7, 50.5, 127.2, 127.9, 129.0, 136.6, 141.0, 161.7, 165.2; MS (CI): m/z = 326 [M+H]$^+$. IR (KBr, cm^{-1}), ν: 3396.7, 1647.8, 1570.0, 1438.6, 1221.4, 1221.4, 862.2, 701.9. EI-HRMS (M + H)$^+$ found 326.0958, calculated for $C_{17}H_{16}N_3O_2S$ 326,0958.

*4.1.4. N-benzyl-4-hydroxy-1,2,5-thiadiazole-3-carboxamide (**4**)*

Obtained using the same procedure as for 3, but using benzylamine instead of 2,2-diphenylethanamine and by heating the reaction mixture at 60 °C¶. Pale yellow solid (m.p. 105.3–106.0 °C from with diisopropyl ether). Yield 83%; 1H NMR (300 MHz, CDCl3, ppm), δ 4.65 (d, J = 6.1 Hz, 2H—CH2Ph), 7.49–7.29 (m, 5H). Exchangeable proton signals overlapped with the water signal.; 13C NMR (75 MHz, CDCl3, ppm), δ 43.5, 127.9, 128.1, 129.0, 136.5, 136.7, 161.7, 165.3; MS (CI): m/z = 236 [M+H]+.IR (KBr, cm-1), ν: 3395, 3367, 1653, 1559, 1437, 1319, 1185, 986, 854, 733. EI-HRMS (M + H)+ found 236.0488, calculated for C10H10N3O2S 236,0488.

*4.1.5. 3-Benzyloxy-N-(2,2-diphenylethyl)-1-methyl-1H-pyrazole-4-carboxamide (**13**)*

A solution of 3-(benzyloxy)-1-methyl-1*H*-pyrazole-4-carboxylic acid (compound **11** [27], 100 mg, 0.431 mmol), 2,2-diphenylethanamine (85.0 mg, 0.431 mmol), DMAP (52.6 mg, 0.431 mmol), and HBTU (327 mg, 0.862 mmol), was stirred at room temperature overnight in dry DMF (15 mL). The solution was concentrated under reduced pressure, resuspended with diethyl ether (50 mL), and washed with 2N HCl (2 × 30 mL). The organic layer was dried over anhydrous Na_2SO_4 and concentrated under reduced pressure to afford the title compound as a pale yellow solid (m.p. 90.2–91.4 °C with diisopropyl ether). Yield 89%. ^{1}H NMR (300 MHz, $CDCl_3$, ppm) δ 3.71 (s; 3H—NCH_3), 3.97 (dd, J = 7.7 Hz and J = 5.8 Hz; 2H —CH_2CH(Ph)$_2$), 4.19 (t, J = 7.9 Hz; 1H—CH$_2$CH(Ph)$_2$), 5.13 (s; 2H—OCH_2Ph), 6.75 (t, J = 5.1 Hz; 1H, —CH$_2$NHCO—), 7.12–7.41 (*m*; 15H, *aromatic protons*), 7.69 (s; 1H, *pyrazole aromatic proton*). ^{13}C NMR (75 MHz, $CDCl_3$, ppm), δ 39.3, 43.4, 50.6, 71.1, 102.8, 126.7, 127.9, 128.0, 128.2, 128.5, 128.6, 134.3, 136.2, 142.1, 159.2, 162.2. MS (CI): m/z = 412 [M+H]$^+$. IR (KBr, cm^{-1}), ν: 3402.0, 1646.2, 1577.0, 1485.4, 1273.1, 1172.5, 965.1.

*4.1.6. 3-Benzyloxy-N-(2,2-diphenylethyl)-1,5-dimethyl-1H-pyrazole-4-carboxamide (**14**)*

Obtained using the same procedure as **13**, starting from 3-(benzyloxy)-1,5-dimethyl-1*H*-pyrazole-4-carboxylic acid (compound **12,** [15])White solid (m.p. 112.3–114.7 °C with diisopropyl ether). Yield 87%. ^{1}H NMR (300 MHz, $CDCl_3$, ppm) δ 2.50 (s, 3H, —CH_3), 3.59 (s, 3H, —NCH_3), 3.97 (dd, J = 7.7 Hz and J = 5.7 Hz; 2H —CH_2CH(Ph)$_2$), 4.19 (t, J = 7.8 Hz; 1H—CH$_2$CH(Ph)$_2$), 5.13 (s; 2H—OCH_2Ph), 6.95 (t, J = 5.0 Hz, 1H, —CH$_2$NHCO—), 7.11–7.46 (m, 15H, a*romatic protons).* ^{13}C NMR (75 MHz, $CDCl_3$, ppm), δ 11.0, 35.4, 43.4, 50.6, 70.7, 98.6, 126.0, 126.6, 127.9, 128.0, 128.5, 128.6, 136.3, 142.1, 144.2, 159.0, 163.8. MS (CI): m/z = 426 [M+H]$^+$. IR (KBr, cm^{-1}), ν: 3389.0, 2941.6, 1639.1, 1560.2, 1438.1, 1310.2, 1095.0, 976.5.

*4.1.7. N-(2,2-diphenylethyl)-3-hydroxy-1-methyl-1H-pyrazole-4-carboxamide (**5**)*

Pd/C (15 mg), was added to a solution of compound **13** (0.100 g, 0.243 mmol), in dry THF (10 mL), and the reaction mixture was stirred under a hydrogen atmosphere for 24 h. The reaction mixture was filtered off through a short layer of celite. The filtrate was evaporated and the resulting product was purified using flash chromatography (eluent DCM/MeOH 95:5 v/v), to give **26** as a white solid (m.p. 239.6–239.8 °C with diisopropyl ether). Yield 88%. ^{1}H NMR (300 MHz, DMSO-d_6, ppm) δ 3.65 (s; 3H—NCH_3), 3.92 (dd J = 7.4 Hz and J = 6.1 Hz, 2H —CH_2CH(Ph)$_2$), 4.27 (t, J = 7.6 Hz, 1H —CH$_2$CH(Ph)$_2$), 7.17–7.29 (m, 10H *aromatic protons*), 7.69 (s, 1H, *pyrazole aromatic proton*), 7.92 (s, 1H, —CH$_2$NHCO—), 10.56 (very br s, 1H, —OH). ^{13}C NMR (75 MHz, DMSO-d_6, ppm), δ 38.8, 43.0, 50.5, 100.9, 126.4, 127.9, 128.4, 132.5, 142.4, 159.6, 162.9. MS (CI): m/z = 322 [M+H]$^+$. IR (KBr, cm^{-1}), ν: 3380.3, 3027.8, 1637.2,

1595.6, 1498.1, 1277.8, 1182.7, 1015.8. EI-HRMS $(M + H)^+$ found 322.1550, calculated for $C_{19}H_{20}N_3O_2$ 322.1550.

*4.1.8. N-(2,2-diphenylethyl)-3-hydroxy-1,5-dimethyl-1H-pyrazole-4-carboxamide (**6**)*

Obtained using the same procedure as **5**, but from **14**White solid (m.p. 245.8–246.5 °C, from diisopropyl ether). Yield 51%. ^{1}H NMR (300 MHz, DMSO-d_6, ppm), δ 2.40 (s, 3H, —CH_3), 3.48 (s; 3H—NCH_3), 3.80–3.94 (m; 2H, —CH_2CH(Ph)$_2$), 4.25 (t, J=7.8 Hz; 1H —CH$_2$CH(Ph)$_2$), 7.19–7.39 (m, 10H, *aromatic protons)*; 11.05 (very br s, 1H, —OH). ^{13}C NMR (75 MHz, DMSO-d_6, ppm), δ 10.3, 35.8, 42.1, 50.3, 97.5, 126.3, 127.8, 128.5, 142.5, 142.7, 158.0, 162.8. MS (CI): m/z = 336 $[M+H]^+$. IR (KBr, cm^{-1}), ν: 3385.7, 3027.2, 1645.9, 1578.1, 1522.5, 1492.1, 1276.0, 1187.7. EI-HRMS $(M + H)^+$ found 336.1707, calculated for $C_{20}H_{22}N_3O_2$ 336.1706.

*4.1.9. Ethyl 3-((tert-butoxycarbonyl)oxy)-1,5-dimethyl-1H-pyrazole-4-carboxylate (**16**)*

Cs_2CO_3 (0.885 g, 2.72 mmol), and tert-butoxycarbonyl anhydride (0.593 g, 2.72 mmol), were added to a solution of **15** [15], (0.500 g, 2.72 mmol), in dry THF (35 mL). The reaction mixture was stirred under reflux for 4 h and allowed to reach room temperature. The solvent was concentrated under reduced pressure and the residue was dissolved in water (50 mL), and extracted with diethyl ether (3 × 50 mL). The combined organic layer was washed with brine, dried over anhydrous Na_2SO_4 and concentrated under reduced pressure. The residue was purified by column chromatography (petroleum ether/ethyl acetate 80:20 v/v), to afford the title compound **16** as a white solid (m.p. 87.9–89.0 °C). Yield 72%. ^{1}H NMR (300 MHz, $CDCl_3$, ppm), δ: 1.33 (t, J=7.14 Hz, 3H, —CH$_2$CH_3), 1.56 (s, 9H, —C(CH_3)$_3$), 2.52 (s, 3H, —CH_3), 3.74 (s, 3H, —NCH_3), 4.27 (q, J=7.14 Hz, 2H, —CH_2CH$_3$). ^{13}C NMR (75 MHz, $CDCl_3$, ppm), δ: 11.22, 14.35, 27.63, 36.27, 59.92, 84.03, 101.78, 144.94, 150.73, 153.78, 162.30; MS (CI): m/z = 285 $[M+H]^+$; MS (EI): m/z=284, 211, 184, 138 (100%). IR (KBr, cm^{-1}), ν: 2989.9, 1763.1, 1705.9, 1558.0, 1482.2, 1366.4, 1314.2, 1251.5, 1153.7.

*4.1.10. Ethyl 5-(bromomethyl)-3-((tert-butoxycarbonyl)oxy)-1-methyl-1H-pyrazole-4-carboxylate (**17**)*

N-bromosuccinimide (2.16 g, 12.13 mmol), and benzoyl peroxide (0.242 g, 1.06 mmol), were added to a solution of **16** (3.00 g, 10.55 mmol), in dichloroethane (180 mL). The solution was stirred at reflux, under an inert atmosphere for 24 h and the solvent was then evaporated under reduced pressure. The residue was purified by column chromatography (gradient of petroleum ether/ethyl acetate), to afford **17** as a white solid (m.p. 72.0–74.0 °C). Yield: 48%. ^{1}H NMR (300 MHz, $CDCl_3$, ppm), δ: 1.36 (t, J=7.14 Hz, 3H, —CH$_2$CH_3), 1.56 (s, 9 H, —C(CH_3)$_3$), 3.85 (s, 3H, —NCH_3), 4.32 (q, J=7.14 Hz, 2H, —CH_2CH$_3$), 4.77 (s, 2H, —CH_2Br). ^{13}C NMR (75 MHz, $CDCl_3$, ppm) δ: 14.25, 17.98, 27.60, 36.72, 60.49, 84.41, 102.29, 142.59, 150.39, 153.66, 161.41; MS (CI): m/z = 363 $[M+H]^+$; MS (EI): m/z=364, 362, 264–262, 183 (100%), 137. IR (KBr, cm^{-1}), ν: 2983.0, 1761.4, 1704.0, 1559.2, 1262.2, 1155.7.

*4.1.11. General procedure for the synthesis of **18a - f***

Substituted phenols, aniline N-methylaniline and tiophenol (6.61 mmol), were added separately to make solutions with **17** (2.00 g, 5.51 mmol), and caesium carbonate (2.15 g, 6.61 mmol), in dry DMF (50 mL). The reaction mixture was stirred at room temperature, under an inert atmosphere, until the starting material (compound **17**), disappeared and water was then added to the reaction mixture. The resulting precipitate was isolated by filtration, washed with cold hexane and dried to give the desired product. When no precipitation occurred, the mixture was extracted with diethyl ether. The combined organic layer was washed with brine, then dried over anhydrous Na_2SO_4 and concentrated under reduced pressure to afford a crude residue that was purified by column chromatography.

*4.1.11.1. Ethyl 3-((tert-butoxycarbonyl)oxy)-1-methyl-5-(phenoxymethyl)-1H-pyrazole-4-carboxylate (**18a**)*

Obtained by precipitation from water. White solid (m.p. 102.3–103.1 °C). Yield 75%. ^{1}H NMR (300 MHz, $CDCl_3$, ppm), δ: 1.33 (t, J=7.14 Hz, 3H, —CH$_2$CH_3), 1.56 (s, 9H, —C(CH_3)$_3$)), 3.91 (s, 3H, —NCH_3), 4.30 (q, J=7.14 Hz, 2H, —CH_2CH$_3$), 5.43 (s, 2H, —CH_2OPh), 6.97–7.05 (m, 3H, *aromatic protons*), 7.31 (t, J=8.23 Hz, 2H, *aromatic protons*); ^{13}C NMR (75 MHz, $CDCl_3$, ppm), δ: 14.26, 27.62, 37.81, 58.88, 60.41, 84.27, 103.08, 114.68, 121.77, 129.65, 142.29, 150.51, 153.64, 157.68, 161.82; MS (CI): m/z = 377 [M+H]+; MS (EI): m/z=376, 276, 183 (100%), 137. IR (KBr, cm^{-1}), ν: 2986.1, 1778.3, 1708.5, 1598.1, 1562.4, 1495.6, 1369.2, 1311.5, 1247.0, 1151.9, 1111.4, 1033.4.

*4.1.11.2. Ethyl 3-((tert-butoxycarbonyl)oxy)-1-methyl-5-((phenylamino)methyl)-1H-pyrazole-4-carboxylate (**18b**)*

Obtained after extraction and column chromatography (gradient of petroleum ether/ethyl acetate). White solid (m.p: 114.2–115.0 °C). Yield 78%. ^{1}H NMR (300 MHz, $CDCl_3$, ppm), δ: 1.31 (t, J=7.12 Hz, 3H, —CH$_2$CH_3), 1.55 (s, 9H, —C(CH_3)$_3$), 3.85 (s, 3H, NCH_3), 4.17 (br s, 1H, NH), 4.28 (q, J=7.12 Hz, 2H, CH_2CH$_3$), 4.54 (s, 2H, CH_2NHPh), 6.71 (d, J=8.50 Hz, 2H, *aromatic protons*), 6.79 (t, J=7.36 Hz, 1H, *aromatic protons*), 7.20 (t, J=7.92 Hz, 2H, *aromatic protons*). ^{13}C NMR (75 MHz, $CDCl_3$, ppm), δ: 14.31, 27.64, 37.16, 38.64, 60.44, 84.33, 102.79, 113.78, 118.91, 129.39, 145.12, 147.34, 150.61, 153.74, 162.07. MS (CI): m/z = 376 $[M+H]^+$. MS (EI): m/z=375, 275, 228 (100%), 137. IR (KBr, cm^{-1}), ν: 3395.9, 2983.4, 1752.4, 1702.3, 1603.7, 1551.3, 1519.7, 1371.4, 1327.5, 1277.8, 1153.3, 1052.0, 906.4, 870.0, 784.4, 748.8, 690.0, 665.8, 513.5.

*4.1.11.3. Ethyl 3-((tert-butoxycarbonyl)oxy)-1-methyl-5-((methyl(phenyl)amino)methyl)-1H-pyrazole-4-carboxylate (**18c**)*

Obtained after extraction and column chromatography (gradient of petroleum ether/ethyl acetate). Yellow solid (m.p: 79.0–80.4 °C). Yield: 74%. 1H NMR (300 MHz, CDCl3, ppm), δ: 1.34 (t, J=7.13 Hz, 3H, —CH2CH3), 1.56 (s, 9H, —C(CH3)3), 2.81 (s, 3H, —NCH3Ph), 3.72 (s, 3H, —NCH3), 4.29 (q, J=7.13 Hz, 2H, —CH2CH3), 4.75 (s, 2H, —CH2NCH3Ph), 6.85 (t, J=7.30 Hz, 1H, aromatic protons), 6.91 (d, J=7.95 Hz, 2H, aromatic protons), 7.30 (t, J=7.39 Hz, 2H, aromatic protons). 13C NMR (75 MHz, CDCl3, ppm), δ: 14.36, 27.66, 37.68, 37.84, 46.33, 60.30, 84.22, 103.46, 114.58, 118.92, 129.39, 144.47, 150.08, 150.61, 153.74, 162.10. MS (CI): m/z = 390 [M+H]+. MS (EI): m/z=389, 289, 228, 137 (100%). IR (KBr, cm-1), ν: 2991.5, 1769.1, 1707.7, 1506.3, 1368.1, 1253.1, 931.7, 892.4, 749.9, 693.0, 643.7, 516.0, 462.4.

*4.1.11.4. Ethyl 3-((tert-butoxycarbonyl)oxy)-1-methyl-5-((phenylthio)methyl)-1H-pyrazole-4-carboxylate (**18d**)*

Obtained after extraction and column chromatography (gradient of petroleum ether/ethyl acetate). White solid (m.p: 113.0–114.0 °C). Yield 64%. ^{1}H NMR (300 MHz, DMSO-d_6, ppm) δ: 1.26 (t, J=7.06, 3H, —CH$_2$CH_3), 1.55 (s, 9H, —C(CH_3)$_3$), 3.60 (s, 3H, —NCH_3), 4.06 (q, J=7.10 Hz, 2H, —CH_2CH$_3$), 4.34 (s, 2H, CH_2SPh), 7.17–7.47 (m, 5H, *aromatic protons*). ^{13}C NMR (75 MHz, DMSO-d_6, ppm), δ: 14.02, 27.12, 27.47, 36.62, 59.78, 83.99, 101.27, 127.87, 129.11, 132.10, 133.16, 143.85, 149.66, 152.86, 160.93. MS (CI):

m/z = 393 $[M+H]^+$. MS (EI): *m/z*=392, 292, 246, 183, 137 (100%). IR (KBr, cm^{-1}), *ν*: 2983.9, 1759.3, 1711.0, 1551.6, 1496.1, 1372.1, 1257.5, 1138.6, 880.2, 763.8, 694.7.

*4.1.11.5. Ethyl 3-((tert-butoxycarbonyl)oxy)-1-methyl-5-((3-(trifluoromethyl) phenoxy) methyl)-1H-pyrazole-4-carboxylate (**18e**)*

Obtained after extraction and column chromatography (gradient of petroleum ether/ethyl acetate). White solid (m.p: 87.3–88.3 °C). Yield: 78%. ^{1}H NMR (300 MHz, $CDCl_3$, ppm) *δ*: 1.25 (t, *J*=7.13 Hz, 3H, —CH_2CH_3), 1.48 (s, 9H, —$C(CH_3)_3$), 3.84 (s, 3H, —NCH_3), 4.23 (q, *J*=7.13 Hz, 2H, —CH_2CH_3), 5.41 (s, 2H, —CH_2OPh), 7.11 (d, *J*=7.21 Hz, 1H, *aromatic protons*), 7.19–7.20 (m, 2H, *aromatic protons*), 7.34 (t, *J*=7.96 Hz, 1H, *aromatic protons*). ^{13}C NMR (75 MHz, $CDCl_3$, ppm), *δ*: 14.37, 27.75, 37.90, 59.03, 60.75, 84.57, 103.53, 111.66 (q, *J*=3.8 Hz), 118.32, 118.63 (q, J=3.9), 123.90 (q, J=272.4), 130.41, 141.22 (q, *J*=32.4 Hz), 141.71, 150.61, 153.89, 157.81, 161.98. MS (CI): *m/z* = 445 $[M+H]^+$. MS (EI): *m/z*=344, 183 (100%), 137.

*4.1.11.6. Ethyl 3-((tert-butoxycarbonyl)oxy)-1-methyl-5-((4-(trifluoromethyl) phenoxy)methyl)-1H-pyrazole-4- carboxylate (**18f**)*

Obtained after extraction and column chromatography (gradient of petroleum ether/ethyl acetate). White solid (mp: 100.6–103.2 °C). Yield: 55%. ^{1}H NMR (300 MHz, $CDCl_3$, ppm), *δ*: 1.32 (t, *J*=7.12 Hz, 3H, —CH_2CH_3), 1.55 (s, 9H, —$C(CH_3)_3$), 3.90 (s, 3H, —NCH_3), 4.30 (q, *J*=7.12 Hz, 2H, —CH_2CH_3), 5.48 (s, 2H, —CH_2OPh), 7.08 (d, *J*=8.65 Hz, 2H, *aromatic protons*), 7.56 (d, *J*=8.72 Hz, 2H, *aromatic protons*). ^{13}C NMR (75 MHz, $CDCl_3$, ppm), *δ*: 14.40, 27.76, 37.91, 59.00, 60.73, 84.59, 103.48, 114.80, 124.10 (q, *J*=33 Hz), 124.34 (q, *J*=271.9 Hz) 127.27 (q, *J*=3.7 Hz), 141.68, 150.63, 153.73, 160.14, 161.98. MS (CI): *m/z* = 445 $[M+H]^+$. MS (EI): *m/z*=344, 183 (100%), 137.

*4.1.12. General procedure for the synthesis of **19a-f***

The appropriate protected compound **18a-f** (2.00 mmol), was dissolved in dry DCM (40 mL). Trifluoroacetic acid (10.00 mmol), was added and the reaction mixture was stirred until the disappearance of starting material was observed. The reaction mixture was quenched with water, the layers were separated and the organic phase was washed with brine and dried with $MgSO_4$. The solvent was evaporated to give the series **19** compounds.

*4.1.12.1. Ethyl 3-hydroxy-1-methyl-5-(phenoxymethyl)-1H-pyrazole-4-carboxylate (**19a**)*

White solid (m.p: 147.5–148.3 °C, from diethyl ether). Yield: 79%. ^{1}H NMR (300 MHz, $CDCl_3$, ppm), *δ*: 1.34 (t, *J*=7.14 Hz, 3H, —CH_2CH_3), 3.82 (s, 3H, —NCH_3), 4.37 (q, *J*=7.14 Hz, 2H, —CH_2CH_3), 5.30 (s, 2H, CH_2OPh), 6.95–7.07 (m, 3H, *aromatic protons*), 7.32 (t, *J*=7.68 Hz, 2H, *aromatic protons*), 7.52 (br s, 1H, O*H*). ^{13}C NMR (75 MHz, $CDCl_3$, ppm), *δ*: 14.21, 37.07, 59.05, 60.71, 96.18, 114.69, 121.82, 129.61, 139.36, 157.64, 162.20, 164.95. MS (CI): *m/z* = 277 $[M+H]^+$. MS (EI): *m/z*=276, 183, 137 (100%). IR (KBr, cm^{-1}), *ν*: 2981.7 (broad), 1695.0, 1549.3, 1347.0, 1239.9, 1124.5. ESI-HRMS (*m/z*) $[M + H]^+$ found 277.1181, calculated for $C_{14}H_{17}N_2O_4$ 277.1183.

*4.1.12.2. Ethyl 3-hydroxy-1-methyl-5-((phenylamino)methyl)-1H-pyrazole-4-carboxylate (**19b**)*

White solid (m.p: 159.5–161.0 °C, from ethanol). Yield: 96%. ^{1}H NMR (300 MHz, $CDCl_3$, ppm), *δ*: 1.33 (t, *J*=7.12 Hz, 3H, —CH_2CH_3), 3.77 (s, 3H, —NCH_3), 4.05 (br s, 1H, —N*H*—), 4.35 (q, *J*=7.12 Hz, 2H, —CH_2CH_3), 4.47 (s, 2H, —CH_2NHPh), 6.70 (d, *J*=7.88 Hz, 2H, *aromatic protons*), 6.80 (t, *J*=7.35 Hz, 1H, *aromatic protons*), 7.21 (t, *J*=7.9 Hz, 2H, *aromatic protons*), 8.37 (br s, 1H, O*H*). ^{13}C NMR (75 MHz, $CDCl_3$, ppm), *δ*: 14.35, 36.69, 38.76, 60.76, 95.79, 113.62, 118.95, 129.42, 142.21, 147.25, 162.36, 165.16. MS (CI): *m/z* = 276 $[M+H]^+$. MS (EI): *m/z*=275, 246, 228 (100%), 137. IR (KBr, cm^{-1}), *ν*: 3362.5, 2982.1, 1706.1, 1603.9, 1522.3, 1378.1, 1324.0, 1278.2, 1161.2, 1123.6, 1017.1, 831.7, 785.9, 758.1, 699.3, 636.0, 509.9. ESI-HRMS (*m/z*) $[M + H]^+$ found 276.1344 calculated for $C_{14}H_{19}N_3O_3$ 276.1343.

*4.1.12.3. Ethyl 3-hydroxy-1-methyl-5-((methyl(phenyl)amino)methyl)-1H-pyrazole-4-carboxylate (**19c**)*

White solid (m.p: 136.7–138.0 °C, from diethyl ether). Yield: 89%. ^{1}H NMR (300 MHz, $CDCl_3$, ppm), *δ*: 1.35 (t, *J*=7.13 Hz, 3H, —CH_2CH_3), 2.80 (s, 3H, —NCH_3Ph), 3.64 (s, 3H, —NCH_3), 4.36 (q, *J*=7.13 Hz, 2H, —CH_2CH_3), 4.62 (s, 2H, —CH_2NCH_3Ph), 6.74–7.00 (m, 3H, *aromatic protons*), 7.18–7.39 (m, 2H, *aromatic protons*), 8.44 (br s, 1H, O*H*). ^{13}C NMR (75 MHz, $CDCl_3$, ppm), *δ*: 14.41, 37.10, 37.82, 46.66, 60.69, 96.55, 114.57, 119.00, 129.39, 141.40, 150.01, 162.50, 165.62. MS (CI): *m/z* = 290 $[M+H]^+$. MS (EI): *m/z*=289, 274, 228 (100%), 137. IR (KBr, cm^{-1}), *ν*: 2982.2, 1699.8, 1541.4, 1375.7, 1347.3, 1272.4, 1116.0, 1027.6, 949.6, 840.2, 794.0, 769.9, 751.0, 691.0, 666.2, 626.3, 523.6. ESI-HRMS (*m/z*) $[M + H]^+$ found 290.1504 calculated for $C_{15}H_{20}N_3O_3$ 290.1499.

*4.1.12.4. Ethyl 3-hydroxy-1-methyl-5-((phenylthio)methyl)-1H-pyrazole-4-carboxylate (**19d**)*

White solid (m.p: 128.4–130.0 °C from diethyl ether). Yield: 90%. ^{1}H NMR (300 MHz, DMSO-d_6, ppm), *δ*: 1.18 (t, *J*=7.0 Hz, 3H, —CH_2CH_3), 3.49 (s, 3H, —NCH_3), 4.08 (q, *J*=7.1 Hz, 2H, —CH_2CH_3), 4.45 (s, 2H, —CH_2SPh), 7.30–7.38 (m, 5H, *aromatic protons*), 10.03 (bs, 1H, O*H*). ^{13}C NMR (75 MHz, DMSO-d_6, ppm), *δ*: 14.23, 27.40, 35.89, 59.05, 95.87, 127.47, 129.05, 131.41, 133.90, 141.08, 160.04, 162.65. MS (CI): *m/z* = 293 $[M+H]^+$. MS (EI): *m/z*=292, 183, 137 (100%). IR (KBr, cm^{-1}), *ν*: 2978.6, 1695.9, 1541.0, 1505.4, 1479.4, 1413.9, 1375.2, 1350.3, 1271.5, 1226.9, 1194.0, 1137.9, 1103.2, 1019.9, 852.9, 790.0, 748.2, 689.9, 653.9, 490.4. ESI-HRMS (*m/z*) $[M + H]^+$ found 293.0959 calculated for $C_{14}H_{18}N_2O_3S$ 293.0954.

*4.1.12.5. Ethyl 3-hydroxy-1-methyl-5-((3-(trifluoromethyl)phenoxy)methyl)-1H-pyrazole-4-carboxylate (**19e**)*

White solid (m.p: 127.7–128.4 °C, from diethyl ether). Yield: 64%. ^{1}H NMR (300 MHz, $CDCl_3$, ppm), *δ*: 1.35 (t, *J*=7.14 Hz, 3H, —CH_2CH_3), 3.84 (s, 3H, —NCH_3), 4.39 (q, *J*=7.14 Hz, 2H, —CH_2CH_3), 5.37 (s, 2H, —CH_2OPh), 7.17 (d, *J*=9.05 Hz, 1H, *aromatic proton*), 7.29–7.30 (d and s, 2H, *aromatic protons*), 7.44 (t, *J*=8.21 Hz, 1H, *aromatic proton*), 8.35 (br s, 1H, O*H*). ^{13}C NMR (75 MHz, $CDCl_3$, ppm), *δ*: 14.32, 37.27, 59.29, 61.10, 96.51, 111.51 (q, *J*=3.9 Hz), 118.59, 118.71 (q, *J*=3.9 Hz), 123.90 (q, *J*=271.2 Hz), 130.42, 132.17 (q, *J*=28.5 Hz), 138.64, 157.82, 162.36, 164.94. MS (CI): *m/z* = 345 $[M+H]^+$. MS (EI): *m/z*=344, 183, 155, 137 (100%). IR (KBr, cm^{-1}), *ν*: 2993.81, 2638.56, 1699.17, 1340.31, 1164.30, 1123.08, 1031.61, 881.73, 794.04, 782.53, 695.80. EI-HRMS $[M+H]^+$ found 345.1047, calculated for $C_{15}H_{16}F_3N_2O_4$ 345.1057.

*4.1.12.6. Ethyl 3-hydroxy-1-methyl-5-((4-(trifluoromethyl)phenoxy)methyl)-1H-pyrazole-4-carboxylate (**19f**)*

White solid (m.p: 145.4–146.3 °C, from diethyl ether). Yield: 84%. ^{1}H NMR (300 MHz, $CDCl_3$, ppm), *δ*: 1.33 (t, *J*=7.12 Hz, 3H, —CH_2CH_3), 3.81 (s, 3H, —NCH_3), 4.37 (q, *J*=7.12 Hz, 2H, —CH_2CH_3), 5.34 (s, 2H, —CH_2OPh), 7.06 (d, *J*=8.61 Hz, 2H, *aromatic protons*), 7.57 (d, *J*=8.65 Hz, 2H, *aromatic protons*), 8.29 (br

s, 1H, O*H*). ^{13}C NMR (75 MHz, $CDCl_3$, ppm), δ: 14.44, 37.30, 59.27, 61.05, 96.55, 114.82, 124.32 (q, J=271.40 Hz), 124.70 (q, J=33.75 Hz), 127.29 (q, J=3.75 Hz), 138.61, 160.21, 162.36, 164.97. MS (CI): m/z = 345 $[M+H]^+$. MS (EI): m/z=344, 183, 155, 137 (100%). IR (KBr, cm^{-1}), ν: 2984.91, 2637.88, 1700.75, 1542.57, 1335.23, 1240.95, 1112.47, 836.31. EI-HRMS $[M+H]^+$ found 345.1052, calculated for $C_{15}H_{16}F_3N_2O_4$ 345.1057.

4.1.13. General procedure for the synthesis of ***7a-f***

5M NaOH (3 eq.), was added to a solution of the appropriate ester in ethanol. The solution was stirred for 2–5 h at room temperature, then neutralized with 6M HCl and concentrated under reduced pressure. 2M HCl was added at 0 °C until pH 2 was reached and the resulting suspension was filtered to afford the corresponding acid.

*4.1.13.1. 3-Hydroxy-1-methyl-5-(phenoxymethyl)-1H-pyrazole-4-carboxylic acid (**7a**)*

White solid (m.p: 171.1–172.5 °C). Yield: 67%. ^{1}H NMR (300 MHz, DMSO-d_6, ppm), δ: 3.66 (s, 3H, —NCH_3), 5.35 (s, 2H, —CH_2OPh), 6.97 (t, J=7.14 Hz, 1H, *aromatic protons*), 7.04 (d, J=7.96 Hz, 2H, *aromatic protons*), 7.31 (t, J=7.96 Hz, 2H, *aromatic protons*). Exchangeable proton signals overlapped with the water signal. ^{13}C NMR (75 MHz, $(CD_3)_2CO$, ppm) δ: 37.22, 59.56, 96.93, 115.67, 122.35, 130.46, 140.89, 159.04, 163.05, 166.76. MS (CI): m/z = 249 $[M+H]^+$. MS (EI): m/z=248, 204, 155, 137, 111. IR (KBr, cm^{-1}), ν: 3079.4 (broad), 1651.9, 1585.8, 1495.5, 1226.0. EI-HRMS $[M+H]^+$ found 249.0865, calculated for $C_{12}H_{14}N_2O_4$ 249.0870.

*4.1.13.2. 3-Hydroxy-1-methyl-5-((phenylamino)methyl)-1H-pyrazole-4-carboxylic acid (**7b**)*

White solid (m.p: 174.5–175.7 °C, from methanol). Yield: 87%. ^{1}H NMR (300 MHz, DMSO-d_6, ppm), δ: 3.62 (s, 3H, —NCH_3), 4.46 (s, 2H, —CH_2NHPh), 6.56 (t, J=7.3 Hz, 1H, *aromatic protons*), 6.66 (d, J=7.8 Hz, 2H, *aromatic protons*), 7.06 (t, J=7.8 Hz, 2H, *aromatic protons*). Exchangeable proton signals could be overlapped to the water signal. ^{13}C NMR (75 MHz, DMSO-d_6, ppm), δ: 36.39, 36.39, 96.55, 112.33, 116.42, 128.91, 143.54, 148.19, 160.61, 165.22. MS (CI): m/z = 204 $[M + H—CO_2]^+$. MS (EI): m/z=247, 203, 137, 111 (100%). IR (KBr, cm^{-1}), ν: 3379.5, 3316.9, 3023.2, 1676.6, 1606.3, 1570.4, 1498.6, 1314.7, 1256.0, 1169.5, 1124.2, 1020.3, 923.8, 778.3, 750.9, 725.8, 689.9, 632.0, 510.0. EI-HRMS $[M+H]^+$ found 248.1034, calculated for $C_{12}H_{15}N_3O_3$ 248.1030.

*4.1.13.3. 3-Hydroxy-1-methyl-5-((methyl(phenyl)amino)methyl)-1H-pyrazole-4-carboxylic acid (**7c**)*

Brownish solid (m.p: 157.0–158.9 °C, from petroleum ether). Yield: 85%. ^{1}H NMR (300 MHz, DMSO-d_6, ppm), δ: 2.76 (s, 3H, —NCH_3Ph), 3.51 (s, 3H, —NCH_3), 4.71 (s, 2H, —CH_2NCH$_3$Ph), 6.73 (t, J=7.10 Hz, 1H, *aromatic protons*), 6.92 (d, J=8.16 Hz, 2H, *aromatic protons*), 7.20 (t, J=7.81 Hz, 2H, *aromatic protons*), 9.84 (br s, 1H, —O*H*), 12.42 (br s, 1H, —O*H*). ^{13}C NMR (75 MHz, DMSO-d_6, ppm), δ: 36.66, 37.49, 45.40, 97.30, 113.72, 117.64, 129.02, 142.71, 149.70, 160.54, 165.14. MS (CI): m/z = 262 $[M+H]^+$. MS (EI): m/z=261, 217, 137, 111 (100%). IR (KBr, cm^{-1}), ν: 2870.4, 1675.6, 1560.4, 1498.4, 1326.4, 1174.1, 1123.9, 929.1, 810.1, 789.8, 756.0, 722.7, 695.1, 528.0. ESI-HRMS (m/z) $[M + H]^+$ found 262.1190 calculated for $C_{13}H_{17}N_3O_3$ 262.1186.

*4.1.13.4. 3-Hydroxy-1-methyl-5-((phenylthio)methyl)-1H-pyrazole-4-carboxylic acid (**7d**)*

White solid (m.p: 163.1–164.0 °C). Yield: 88%. ^{1}H NMR (300 MHz, DMSO-d_6, ppm), δ: 3.48 (s, 3H, —NCH_3), 4.47 (s, 2H, —CH_2SPh), 7.17–7.51 (m, 5H, *aromatic protons*), 9.82 (br s, 1H, —O*H*), 12.24 (br s, 1H, —O*H*). ^{13}C NMR (75 MHz, DMSO-d_6, ppm), δ: 26.96, 35.86, 96.13, 127.23, 129.08, 130.79, 134.20, 141.80, 160.48, 164.65. MS (CI): m/z = 221 $[M + H—CO_2]^+$. MS (EI): m/z=264, 246, 155, 137 (100%). IR (KBr, cm^{-1}), ν: 3004.5, 1651.1, 1566.9, 1469.7, 1416.0, 1309.6, 1196.0, 1152.0, 1120.8, 950.4, 772.2, 695.6, 552.2, 499.4. ESI-HRMS (m/z) $[M + H]^+$ found 265.0647 calculated for $C_{12}H_{14}N_2O_3S$ 265.0641.

*4.1.13.5. 3-Hydroxy-1-methyl-5-((3-(trifluoromethyl)phenoxy)methyl)-1H-pyrazole-4-carboxylic acid (**7e**)*

White solid (m.p: 193.8–194.5 °C from diethyl ether). Yield: 83%. ^{1}H NMR (300 MHz, DMSO-d_6, ppm), δ: 3.69 (s, 3H, —NCH_3), 5.45 (s, 2H, —CH_2OPh), 7.32–7.37 (m, 2H, *aromatic protons*), 7.42 (s, 1H, *aromatic protons*), 7.55 (t, J=7.9 Hz, 1H, *aromatic protons*), 10.06 (br s, 1H, —O*H*), 12.46 (br s, 1H, —O*H*). ^{13}C NMR (75 MHz, DMSO-d_6, ppm), δ: 36.41, 58.71, 97.27, 110.99 (q, J=3.75 Hz), 117.70 (q, J=3.68 Hz), 119.14, 123.87 (q, J=270.75 Hz), 130.28 (q, J=31.5 Hz), 130.74, 139.72, 157.89, 160.38, 164.49. IR (KBr, cm^{-1}), ν: 2629.90, 1662.13, 1581.56, 1327.75, 1271.01, 1168.12, 1122.62, 1019.98, 888.83, 872.04, 801.62. EI-HRMS $[M+H]^+$ found 317.0744, calculated for $C_{13}H_{13}F_3N_2O_4$ 317.0744.

*4.1.13.6. 3-Hydroxy-1-methyl-5-((4-(trifluoromethyl)phenoxy)methyl)-1H-pyrazole-4-carboxylic acid (**7f**)*

White solid (m.p: 189.6–190.5 °C from DCM). Yield: 70%. ^{1}H NMR (300 MHz, DMSO-d_6, ppm), δ: 3.69 (s, 3H, —NCH_3), 5.45 (s, 2H, —CH_2OPh), 7.25 (d, J=8.55 Hz, 2H, *aromatic protons*), 7.69 (d, J=8.65 Hz, 2H, *aromatic protons*), 10.07 (br s, 1H, —O*H*), 12.37 (br s, 1H, —O*H*). ^{13}C NMR (75 MHz, DMSO-d_6, ppm), δ: 36.38, 58.73, 97.21, 115.08, 121.69 (q, J=32.1 Hz), 124.39 (q, J=271.1 Hz), 126.97 (q, J=3.8), 139.62, 160.40, 160.55, 164.43. MS (CI): m/z = 317 $[M+H]^+$. MS (EI): m/z=316, 272, 111, 44 (100%). IR (KBr, cm^{-1}), ν: 3518.59, 3014.75, 1655.00, 1331.79, 1166.05, 1112.51, 1068.08, 1011.67, 835.45. EI-HRMS $[M+H]^+$ found 317.0743, calculated for $C_{13}H_{12}F_3N_2O_4$ 317.0744.

4.1.14. General procedure for the synthesis of ***21a-c***

Compound **19a** (1.08 mmol), was dissolved in either acetonitrile or DMF (35 mL or 5 mL). Potassium carbonate (2.7 mmol), and either alkyl or benzyl halides (1.19 mmol), were added. The reaction mixture was stirred at 50 °C, until the disappearance of the starting material was observed. It was then concentrated under reduced pressure and the residue was partitioned between ethyl acetate and water. The organic layer was washed with 1M NaOH, brine, dried over $MgSO_4$ and concentrated under reduced pressure. The crude product was purified by column chromatography (gradient of petroleum ether/ethyl acetate), to give the series **21** compounds.

*4.1.14.1. Ethyl 3-ethoxy-1-methyl-5-(phenoxymethyl)-1H-pyrazole-4-carboxylate (**21a**)*

White solid (m.p: 74.8–75.4 °C). Yield: 71%. The reaction was performed in acetonitrile for 48 h, using iodoethane as the alkyl halide. ^{1}H NMR (300 MHz, $CDCl_3$, ppm), δ: 1.32 (t, J=7.1, 3H, —CH$_2$CH_3), 1.43 (t, J=7.0, 3H, —OCH$_2$CH_3), 3.80 (s, 3H, —NCH$_3$), 4.29 (q, J=7.0 Hz, 2H, —OCH_2CH$_3$), 4.30 (q, J=7.1 Hz, 2H, —CH_2CH$_3$), 5.41 (s, 2H, —CH_2OPh), 6.95–7.03 (m, 3H, *aromatic protons*), 7.18–7.43 (m, 2H, *aromatic protons*). ^{13}C NMR (75 MHz, $CDCl_3$, ppm), δ: 14.29, 14.70, 37.20, 59.09, 60.01, 64.94, 98.10, 114.74, 121.61, 129.62, 141.70, 157.77, 161.48, 163.13. MS (CI): m/z = 305 $[M+H]^+$. MS (EI): m/z=304, 211, 183, 137 (100). IR (KBr,

cm^{-1}), ν: 2987.31, 2902.21, 1706.12, 1508.66, 1230.49, 1125.70, 871.28, 760.56.

*4.1.14.2. Ethyl 3-(cyclopropylmethoxy)-1-methyl-5-(phenoxymethyl)-1H-pyrazole-4-carboxylate (**21b**)*

White solid (m.p: 58.5–59.8 °C). Yield: 67%. The reaction was performed in acetonitrile for 48 h, using (bromomethyl)cyclopropane as the alkyl halide. ^{1}H NMR (300 MHz, $CDCl_3$, ppm), δ: 0.60–0.38 (m, 4H, CH(CH_2)$_2$), 1.01–1.51 (m, 4H, —OCH$_2$*CH*— and —OCH$_2$C*H*$_3$), 3.79 (s, 3H, —NC*H*$_3$), 3.36–4.17 (m, 2H, —O*CH*$_2$-), 4.20–4.46 (m, 2H, —C*H*$_2$CH$_3$), 5.41 (s, 2H, —C*H*$_2$OPh), 6.99–7.29 (m, 5H, *aromatic protons*). ^{13}C NMR (75 MHz, $CDCl_3$, ppm), δ: 3.11, 10.13, 14.27, 37.20, 59.09, 59.99, 73.56, 98.19, 114.75, 121.61, 129.75, 141.76, 157.20, 161.59, 163.16. MS (CI): m/z = 331 $[M+H]^+$. MS (EI): m/z=330, 183, 155, 137 (100%). IR (KBr, cm^{-1}), ν: 2932.28, 1711.21, 1507.52, 1114.11, 758.47.

*4.1.14.3. Ethyl 3-(benzyloxy)-1-methyl-5-(phenoxymethyl)-1H-pyrazole-4-carboxylate (**21c**)*

White solid (m.p: 84.8–85.6 °C). Yield: 71% yield as a white solid. The reaction was performed in DMF for 24 h using benzyl bromide as the benzyl halide. ^{1}H NMR (300 MHz, $CDCl_3$, ppm), δ: 1.34 (t, 3H, J=7.25 Hz, —OCH$_2$C*H*$_3$), 3.82 (s, 3H, —NC*H*$_3$), 4.31 (q, 2H J=7.25 Hz, —OC*H*$_2$CH$_3$), 5.32* (s, 2H, —C*H*$_2$OPh), 5.43* (s, 2H, —OC*H*$_2$Ph), 6.93–7.07 (m, 3H, *aromatic protons*), 7.24–7.44 (m, 5H, *aromatic protons*), 7.50 (d, 2H, J=6.82 Hz, *aromatic protons*). ^{13}C NMR (75 MHz, $CDCl_3$, ppm), δ: 14.27, 37.25, 58.96, 60.02, 70.26, 98.27, 114.71, 121.61, 127.09, 127.64, 128.29, 129.61, 136.97, 142.10, 157.72, 161.04, 163.15. MS (CI): m/z = 367 $[M+H]^+$. MS (EI): m/z=366, 273, 137, 91 (100%). IR (KBr, cm^{-1}), ν: 2976.5, 1690.4, 1568.1, 1494.2, 1358.3, 1315.9, 1235.7, 1169.3, 1134.5, 1006.4.

*4.1.15. General procedure for the synthesis of **22a-c***

6M NaOH (0.82 mL, 5.0 mmol), was added to an ethanol suspensions of compounds **21a**, **21b** and **21c**. (1.0 mmol). The reaction mixture was stirred at 50 °C until the disappearance of the starting material was observed. 2M HCl was added until the pH reached a value of 7. Ethanol was evaporated and water was added. 2M HCl was added until the pH reached a value of 4. The precipitate was isolated by filtration, washed with water and dried under vacuum to give the series **22** compounds.

*4.1.15.1. 3-Ethoxy-1-methyl-5-(phenoxymethyl)-1H-pyrazole-4-carboxylic acid (**22a**)*

White solid (m.p: 174.1–175.8 °C). Yield: 68%. ^{1}H NMR (300 MHz, DMSO-d_6, ppm), δ: 1.31 (t, J=7.01 Hz, 3H, —OCH$_2$C*H*$_3$), 3.73 (s, 3H, —NC*H*$_3$), 4.19 (q, J=7.01 Hz, 2H, —OC*H*$_2$CH$_3$), 5.40 (s, 2H, —C*H*$_2$OPh), 6.98 (t, J=7.33 Hz, 1H, *aromatic protons*), 7.04 (d, J=8.13 Hz, 2H, *aromatic protons*), 7.31 (t, J=7.80 Hz, 2H, *aromatic protons*), 12.29 (br s, 1H, —COOH). ^{13}C NMR (75 MHz, DMSO-d_6, ppm), δ: 14.68, 36.80, 58.33, 64.15, 97.79, 114.66, 121.30, 129.63, 141.81, 157.76, 160.60, 163.69. MS (CI): m/z = 277 $[M+H]^+$. MS (EI): m/z=276, 183, 137 (100%). IR (KBr, cm^{-1}), ν: 2977.68, 1654.50, 1031.79, 776.05, 761.42. EI-HRMS $[M+H]^+$ found 277.1185, calculated for $C_{14}H_{17}N_2O_4$ 277.1183.

*4.1.15.2. 3-(Cyclopropylmethoxy)-1-methyl-5-(phenoxymethyl)-1H-pyrazole-4-carboxylic acid (**22b**)*

White solid (m.p: 166.8–168.2 °C). Yield: 78%. ^{1}H NMR (300 MHz, DMSO-d_6, ppm), δ: 0.27–0.36 (m, 2H, —CH(CH_2)$_2$), 0.49–0.59 (m, 2H, —CH(CH_2)$_2$), 1.04–1.51 (m, 1H, —C*H*—), 3.72 (s, 3H, —NCH$_3$), 3.97 (d, J=7.03 Hz, 2H, —C*H*$_2$CH—), 5.40 (s, 2H, —C*H*$_2$OPh), 6.98 (t, J=7.28 Hz, 1H, *aromatic protons*), 7.04 (d, J=8.02 Hz 2H, *aromatic protons*), 7.31 (t, J=7.85 Hz, 2H, *aromatic protons*), 12.31 (br s, 1H, —O*H*). ^{13}C NMR (75 MHz, DMSO-d_6, ppm), δ: 3.22, 10.14, 36.79, 58.31, 72.93, 97.78, 114.65, 121.29, 129.63, 141.82, 157.74, 160.71, 163.69. MS (CI): m/z = 303 $[M+H]^+$. MS (EI): m/z=302, 155, 137 (100%). IR (KBr, cm^{-1}), ν: 2934.08, 1654.80, 1559.85, 1490.62, 1215.72, 1030.81, 760.13. EI-HRMS $[M+H]^+$ found 303.1333, calculated for $C_{16}H_{19}N_2O_4$ 303.1339.

*4.1.15.3. 3-(Benzyloxy)-1-methyl-5-(phenoxymethyl)-1H-pyrazole-4-carboxylic acid (**22c**)*

White solid (m.p: 152.8–153.4 °C). Yield: 91% yield as a white solid. ^{1}H NMR (300 MHz, $CDCl_3$, ppm), δ: 3.83 (s, 3H, —NC*H*$_3$), 5.36* (s, 2H, —OC*H*$_2$Ph), 5.45* (s, 2H, —C*H*$_2$OPh), 6.93–7.05 (m, 3H, *aromatic protons*), 7.23–7.52 (m, 7H, *aromatic protons*). ^{13}C NMR (75 MHz, $CDCl_3$, ppm), δ: 37.68, 58.88, 71.31, 97.41, 114.83, 121.86, 127.98, 128.35, 128.68, 129.81, 136.21, 143.24, 157.64, 160.98, 165.79. MS (CI): m/z = 339 $[M+H]^+$. MS (EI): m/z=338, 245, 137, 91 (100%). IR (KBr, cm^{-1}), ν: 2937.5, 1653.0, 1564.2, 1495.4, 1224.4, 1171.3, 1010.0. EI-HRMS $[M+H]^+$ found 339.1339, calculated for $C_{19}H_{29}N_2O_4$ 339.1339.

*4.1.15.4. 3-(Benzyloxy)-1-methyl-5-(phenoxymethyl)-1H-pyrazole-4-carboxamide (**23**)*

An oxalyl chloride solution 2M in DCM (1.20 mL, 2.40 mmol), and dry DMF (7 µL), were added to a cooled (0 °C), solution of **22c** (0.338 g, 1.00 mmol), in dry THF (30 mL). The reaction mixture was stirred for 2 h at room temperature. The solvent was evaporated and the residue was dissolved in dry THF (10 mL). This solution was slowly added to a concentrated ammonia solution (10 mL). The reaction mixture was diluted with water and extracted twice with ethyl acetate. The combined organic layer was washed with brine, dried over Na_2SO_4 and the solvent was evaporated to give **23** as a white solid (M.p.: 132.5–133.3 °C). Yield 95%. ^{1}H NMR (300 MHz, $CDCl_3$, ppm), δ: 3.83 (s, 3H, —NC*H*$_3$), 5.31*(s, 2H, —C*H*$_2$OPh), 5.58* (s, 2H, —OC*H*$_2$Ph), 5.63 (br s, 1H, —N*H*), 6.83 (br s, 1H, —N*H*), 6.95 (t, J=7.32 Hz, 1H, *aromatic protons*), 7.04 (d, J=8.42 Hz, 2H, *aromatic protons*), 7.22–7.45 ppm (m, 7H, *aromatic protons*). ^{13}C NMR (75 MHz, $CDCl_3$, ppm), δ: 37.31, 58.67, 71.37, 99.20, 114.76, 121.46, 128.20, 128.53, 128.70, 129.60, 135.97, 142.23, 157.62, 159.28, 164.75. MS (CI): m/z = 338 $[M+H]^+$. MS (EI): m/z=337, 244, 137, 91 (100%). IR (KBr, cm^{-1}), ν: 3434.5, 3164.9, 1671.0, 1615.3, 1495.6, 1357.1, 1239.5, 1137.4, 1006.8.

*4.1.15.5. 3-Hydroxy-1-methyl-5-(phenoxymethyl)-1H-pyrazole-4-carboxamide (**24**)*

Pd/C (0.050 g), was added to a solution of compound **23** (0.337 g, 1.00 mmol), in dry THF (15 mL), and the reaction mixture was stirred under a hydrogen atmosphere for 24 h. The reaction mixture was filtered off through a short layer of celite and washed with methanol. The solvent was evaporated and the residue recrystallized from ethanol to give **13** as a white solid (M.p.: 265.5–267 °C). Yield: 77%. ^{1}H NMR (300 MHz, DMSO-d_6, ppm), δ: 3.66 (s, 3H, —NC*H*$_3$), 5.49 (s, 2H, —C*H*$_2$OPh), 6.81 (br s, 1H, —N*H*), 6.95 (t, J=7.27 Hz, 1H, *aromatic protons*), 7.06 (d, J=7.96 Hz, 2H, *aromatic protons*), 7.20 (br s, 1H, —N*H*), 7.29 (t, J=8.23 Hz, 2H, *aromatic protons*), 11.40 (bs, 1H, —O*H*). ^{13}C NMR (75 MHz, DMSO-d_6, ppm), δ: 36.52, 58.47, 99.52, 115.03, 121.52, 129.92, 140.75, 158.16, 158.64, 164.77. MS (CI): m/z = 248 $[M+H]^+$. MS (EI): m/z=247, 154, 137, 44 (100%). IR (KBr, cm^{-1}), ν: 3417.1, 3171.1, 1576.1, 1451.4, 1231.4,

1012.9. EI-HRMS $[M+H]^+$ found 248.1027, calculated for $C_{12}H_{14}N_3O_3$ 248.1030.

4.2. Biological assay

4.2.1. PfDHODH inhibition assay

In order to determine the inhibition and IC_{50} values of *Plasmodium falciparum* DHODH, the recombinant *Pf*DHODH enzymes were used in an *in vitro* enzyme assay with N-terminally truncated recombinant *Pf*DHODH [38]. The assay is based on the coupling of ubiquinone reduction to the redox dye 2,6-dichloroindophenol (DCIP) [39]. The reduction of DCIP was monitored photometrically via decreasing absorption at 600 nm. The test solutions contained 60 μM DCIP, 150 mM KCl, 50 mM TRIS/HCl pH 7.8, 0.1% Triton X-100, 20 μM decylubiquinone and 200 μM DHO. Synthesized compounds were dissolved in DMSO and normally added to a final concentration of 1% DMSO. The reaction was initiated by the addition of DHO, and the initial rate was measured 5 times per minute in the first 5 min. IC_{50} values were calculated using GraphPad Prism software. Values are means ± SE of three independent experiments. A higher concentration of DMSO, 5%, was used to prevent the precipitation and measurement inhibition of compounds with IC50 values of higher than 100 μM. No enzyme function inhibition was found in the 5% DMSO-containing control.

4.2.2. hDHODH inhibition assay

Inhibitory activity was assessed by monitoring the reduction of 2,6-dichloroindophenol (DCIP), which is associated with the DHODH enzyme-catalyzed oxidation of dihydroorotate. The enzyme was pre-incubated for 5 min at 37 °C in Tris-buffer solution (pH 8.0), with coenzyme Q10 (100 μM), the compounds to be tested at a variety of concentrations (final DMSO concentration 0.1% v/v), and DCIP (50 μM). The reaction was initiated by the addition of DHO (500 μM), and reduction was monitored at λ = 650 nm. The initial rate was measured in the first 5 min (ε = 10400 M-1cm-1), and IC_{50} values were calculated, when possible [9], using GraphPad Prism software. Values are means ± SE of three independent experiments.

4.2.3. Human protein expression and purification for inhibition assay

The cDNA of the N-truncated form of *h*DHODH (aa31 - 395), was amplified from a full length *h*DHODH I.M.A.G.E. clone (ID 6064723), and inserted into a pFN2A vector (Promega). The vector produces *h*DHODH as an N-terminal GST-fusion protein. The plasmid pFN2A–*h*DHODH was transformed into BL21 (DE3), pyrD *E. coli* cells for protein production. Cells were grown at 37 °C in LB medium supplemented with 0.1 mM flavin mononucleotide. After 20 h of growth, cells were induced with 0.4 mM isopropyl-D-thiogalactopyranoside at an OD_{600} of 0.6–0.8 at 28 °C for an additional 3 h. A cell pellet from 300 mL of culture was lysed in 20 mL of PBS (50 mM Na_2HPO_4, 50 mM NaH_2PO_4, 500 mM NaCl), supplemented with 24 mg lysozyme and 0.2% v/v protease inhibitor cocktail (Sigma-Aldrich), incubated on ice for 30 min and disrupted by sonication. Triton X-100 was added into the lysate to a final concentration of 1% before centrifugation at 14000×*g* for 40 min at 4 °C. The clarified supernatant was incubated with DNase I (Sigma Aldrich), for 30 min at room temperature, supplemented with 2 mM DTT and filtered through a 0.45 μ*m* syringe filter. The GST-fused enzyme was purified from bacterial lysate by affinity chromatography on immobilized glutathione-sepharose columns using fast protein liquid chromatography (FPLC). The GST tag was not removed to facilitate further study.

4.2.4. Pf protein: cloning, expression and purification for crystallisation and inhibition assays

The gene encoding for PfDHODH were codon optimized for *E. coli* (GeneArt, ThermoFischer Scientific). The gene coding for N-terminally truncated PfDHODH (residues 159–569), was PCR amplified using the forward primer: 5′- TACTTCCAATCCATGTTTGAAAGCTATAATC CGG-3′ and the reversed primer: 5′-TATCCACCTTTACTG TTAGCTTTTGCTGTGTTTGC-3’. Using ligation independent cloning, N-terminal truncated PfDHODH was cloned into the pNIC28−Bsa4 [40], vector, which carries a T7 promoter, N-terminal 6 × His-tag followed by TEV cleavage site. pNIC28-Bsa4 was a gift from Opher Gileadi (Addgene plasmid # 26103). In order to delete the surface loop (amino acids 385–415), the QuikChange II Site- Directed Mutagenesis Kit was used with the primers 5′-CAACATCATGAACGACGAGTTTC TGTGGTTC AACACCA-3′ and 5′-TGGTGTTGA ACCACAGAA ACTCGTCGTTCATGATGTTG- 3’ (p1pfDHOH). The identity of each construct was confirmed by DNA sequencing (Eurofins Genomics).

The p1*pf*DHODH plasmid was transformed into the *E. coli* BL21 (DE3) strain. The strain was grown in Terrific Broth media supplemented with kanamycin (50 μg/mL), induced with IPTG (0.2 mM), at 16 °C overnight under shaking at 220 rpm. Cells were harvested by centrifugation (8000×*g* for 20 min), and resuspended in Buffer A (100 mM HEPES pH 8.0, 150 mM NaCl, 10% (*v/v*) glycerol, 0.05% (*w/v*) THESIT and cOmplete™ EDTA free protease inhibitor tablets, Roche). Cells were lysed using an EmulsiFlex-C3 (AVESTIN), at 20,000 psi. Cell debris was removed at 26,000 g for 30 min. The supernatant was subjected to immobilized metal affinity chromatography and loaded onto a 5 mL HisTrap FF column (GE), equilibrated with Buffer A. The protein was purified with an ÄKTA system, washed with Buffer A and Buffer A complemented with 20 mM imidazole. *pf*DHODH was collected using a linear gradient from 20 mM up to 400 mM imidazole in Buffer A over 20 column volumes. The protein was concentrated using Vivaspin concentrator loaded on a HiLoad 16/600 Superdex 200 size exclusion column equilibrated with 10 mM HEPES, pH 7.8, 150 mM NaCl, 10 mM N,N-dimethyldodecylamine N-oxide, 5% (*v/v*), glycerol and 10 mM dithiothreitol. Protein concentration was determined using a ND-1000 spectrophotometer at 280 nm, using the extinction coefficient of 29,340 $M^{-1}cm^{-1}$ and a molecular weight of 45 kDa. The eluted protein fractions were analyzed using SDS PAGE, wherein bands with the desired protein size were pooled together and concentrated to 30 mg/mL. The protein was used directly for crystallization and was flash frozen in liquid nitrogen and stored at −80 °C until use.

4.2.5. Crystallization, data collection, solution and refinement

*Pf*DHODH (30 mg/mL), was pre-incubated with 2 mM inhibitor and 2 mM orotate prior to crystallization. Sitting-drop vapour diffusion experiments were set up at 20 °C by mixing 1 μl of protein with 1 μl reservoir solution (0.1 M Tris-HCl (pH 7.5–9.5), 35% (*w/v*) PEG 4000 and 50 mM sodium formate), equilibrated over 1 mL of reservoir solution. Needle-shaped crystals of *Pf*DHOHD appeared after one week. For X-ray data collection, the crystals were briefly soaked in cryoprotectant solution that contained reservoir solution made up to 25% (v/v), ethylene glycol before being flash-cooled in liquid nitrogen. Intensity data were collected on the ID29 and MASSIF-2 beamlines at the European Synchrotron Facility (ESRF), France.

4.2.6. Growth inhibition assays against P. falciparum-infected erythrocytes

P. falciparum 3D7 cells were grown in red blood cells (type O+ human erythrocytes, Blood Centre, University of Campinas), in medium that contained RPMI 1640, 25 mM HEPES, pH 7.3, 2 g/litre sodium bicarbonate, 4 mM L-glutamine, 0.2% D-glucose (wt/wt), 22 μg/mL gentamicin and 0.5 mM hypoxantine that was supplemented with 10% human serum. Cultures were kept with 4% hematocrit and incubated at 37 °C in 1% O_2, 5% CO_2 and 94% N_2. In order to generate synchronized ring stage parasites, cultures were synchronized with sorbitol 5% for 10 min of incubation. The tested compounds were serially diluted (1:2), in complete medium with 2% hematocrit either with or without 1–2% parasitemia in a 96 well plate with a starting concentration of 300 μM for each compound, while DMSO concentration was adjusted for all wells. Parasite viability was determined by measuring parasitemia in the parasite life cycle for 48 h following drug treatment by flow cytometry using SybrGreen I (Sigma S9430), to stain infected red blood cells. After 48 h of drug incubation, the culture medium was removed and the cell pellets were resuspended in 15 μL SybrGreen (1:1000 dilution in PBS 1× BSA 0.5%), for 20 min at 25 °C and washed twice with PBS. Data at each concentration point was collected in triplicate and were fitted to the log[I] vs response model in Graph Pad Prism 5 to determine the concentration of inhibitor that resulted in 50% growth inhibition (EC_{50}).

4.2.7. In vitro cytotoxicity assays

In vitro toxicity was assessed in fibroblast-like cell lines derived from monkey kidney tissue (COS-7 cells), cultured in DMEN medium that was supplemented with 10% heat-inactivated fetal bovine serum and 40 mg/L gentamicin in a 5% CO_2 atmosphere at 37 °C. Cells were distributed in a flat bottom 96-microplate (10^4 cells/well), in 100 μL of DMEN medium and incubated for 16 h to ensure cell adherence. Subsequently, the medium was carefully removed and the compounds were added to each well at different concentrations and incubated for 48 h. For the MTT assay, 20 μL of MTT [3-(4,5-dimethylthiazol-2-yl)-2,5-diphenyltetrazolium bromide] (5 mg/mL), were added to each well and they were incubated for 4 h. The supernatant was then removed and 100 μL of MTT (4 mM HCl, 10% Triton X-100 in isopropanol), were added and the plates were covered with tinfoil and agitated on an orbital shaker for 1 h to dissolve the formazan crystals. Optical density was determined at 570 nm (CLARIOstar, Labtech BMG), and the 50% cytotoxicity concentrations (CC_{50}), were expressed as percentage viability relative to the control.

Notes

The authors declare no competing financial interests.

PDB ID codes

The atomic coordinates and structure factors of *Pf*DHODH in complex with compounds **3** (PDB id: 6I55) and **7e** (PDB id: 6I4B) have been deposited in the RCSB Protein Data Bank.

Acknowledgements

This research was supported by funding from the University of Turin, Ricerca Locale 2016 and 2017 (Grant numbers LOLM_RILO_17_01, LOLM_RILO_18_01, BOSD_RILO_17_01 and BOSD_RILO_18_01) and from Ministero degli Affari Esteri e della Cooperazione Internazionale (Grant number PGR00978). FTMC and CHA labs are supported by CNPq and FAPESP grants and they are CNPq research fellows. GCC and TAT received FAPESP (n° 2015/20774-6) and CAPES fellowships, respectively. The authors would like to thank Davide Bonanni for the helpful discussions on the compound binding mode and for preparing the final crystallographic figures, Livio Stevanato for maintaining the NMR instrumentation and Dale James Matthew Lawson for proofreading the final manuscript.

Appendix A. Supplementary data

Supplementary data to this article can be found online at https://doi.org/10.1016/j.ejmech.2018.11.044.

References

[1] M.A. Phillips, J.N. Burrows, C. Manyando, R.H. van Huijsduijnen, W.C. Van Voorhis, T.N.C. Wells, Malaria, Nat Rev Dis Primers 3 (2017) 17050.
[2] J.N. Burrows, S. Duparc, W.E. Gutteridge, R. Hooft van Huijsduijnen, W. Kaszubska, F. Macintyre, S. Mazzuri, J.J. Mohrle, T.N.C. Wells, New developments in anti-malarial target candidate and product profiles, Malar. J. 16 (2017) 26.
[3] A. Singh, M. Maqbool, M. Mobashir, N. Hoda, Dihydroorotate dehydrogenase: a drug target for the development of antimalarials, Eur. J. Med. Chem. 125 (2017) 640–651.
[4] L.V. Hoelz, F.A. Calil, M.C. Nonato, L.C. Pinheiro, N. Boechat, Plasmodium falciparum dihydroorotate dehydrogenase: a drug target against malaria, Future Med. Chem. 10 (2018) 1853–1874.
[5] M.A. Phillips, J. Lotharius, K. Marsh, J. White, A. Dayan, K.L. White, J.W. Njoroge, F. El Mazouni, Y. Lao, S. Kokkonda, D.R. Tomchick, X. Deng, T. Laird, S.N. Bhatia, S. March, C.L. Ng, D.A. Fidock, S. Wittlin, M. Lafuente-Monasterio, F.J. Benito, L.M. Alonso, M.S. Martinez, M.B. Jimenez-Diaz, S.F. Bazaga, I. Angulo-Barturen, J.N. Haselden, J. Louttit, Y. Cui, A. Sridhar, A.M. Zeeman, C. Kocken, R. Sauerwein, K. Dechering, V.M. Avery, S. Duffy, M. Delves, R. Sinden, A. Ruecker, K.S. Wickham, R. Rochford, J. Gahagen, L. Iyer, E. Riccio, J. Mirsalis, I. Bathhurst, T. Rueckle, X. Ding, B. Campo, D. Leroy, M.J. Rogers, P.K. Rathod, J.N. Burrows, S.A. Charman, A long-duration dihydroorotate dehydrogenase inhibitor (DSM265) for prevention and treatment of malaria, Sci. Transl. Med. 7 (2015), 296ra111.
[6] J.S. McCarthy, J. Lotharius, T. Ruckle, S. Chalon, M.A. Phillips, S. Elliott, S. Sekuloski, P. Griffin, C.L. Ng, D.A. Fidock, L. Marquart, N.S. Williams, N. Gobeau, L. Bebrevska, M. Rosario, K. Marsh, J.J. Mohrle, Safety, tolerability, pharmacokinetics, and activity of the novel long-acting antimalarial DSM265: a two-part first-in-human phase 1a/1b randomised study, Lancet Infect. Dis. 17 (2017) 626–635.
[7] A. Llanos-Cuentas, M. Casapia, R. Chuquiyauri, J.C. Hinojosa, N. Kerr, M. Rosario, S. Toovey, R.H. Arch, M.A. Phillips, F.D. Rozenberg, J. Bath, C.L. Ng, A.N. Cowell, E.A. Winzeler, D.A. Fidock, M. Baker, J.J. Mohrle, R. Hooft van Huijsduijnen, N. Gobeau, N. Araeipour, N. Andenmatten, T. Ruckle, S. Duparc, Antimalarial activity of single-dose DSM265, a novel plasmodium dihydroorotate dehydrogenase inhibitor, in patients with uncomplicated Plasmodium falciparum or Plasmodium vivax malaria infection: a proof-of-concept, open-label, phase 2a study, Lancet Infect. Dis. 18 (2018) 874–883.
[8] S. Kokkonda, F. El Mazouni, K.L. White, J. White, D.M. Shackleford, M.J. Lafuente-Monasterio, P. Rowland, K. Manjalanagara, J.T. Joseph, A. Garcia-Perez, J. Fernandez, F.J. Gamo, D. Waterson, J.N. Burrows, M.J. Palmer, S.A. Charman, P.K. Rathod, M.A. Phillips, Isoxazolopyrimidine-based inhibitors of plasmodium falciparum dihydroorotate dehydrogenase with antimalarial activity, ACS Omega 3 (2018) 9227–9240.
[9] M. Giorgis, M.L. Lolli, B. Rolando, A. Rao, P. Tosco, S. Chaurasia, D. Marabello, R. Fruttero, A. Gasco, 1,2,5-Oxadiazole analogues of leflunomide and related compounds, Eur. J. Med. Chem. 46 (2011) 383–392.
[10] M.L. Lolli, S. Sainas, A.C. Pippione, M. Giorgis, D. Boschi, F. Dosio, Use of human dihydroorotate dehydrogenase (hDHODH) inhibitors in autoimmune diseases and new perspectives in cancer therapy, Recent Pat. Anti-Cancer Drug Discov. 13 (2018) 86–105.
[11] S. Bonomo, P. Tosco, M. Giorgis, M. Lolli, R. Fruttero, The role of fluorine in stabilizing the bioactive conformation of dihydroorotate dehydrogenase inhibitors, J. Mol. Model. 19 (2013) 1099–1107.
[12] S. Sainas, A.C. Pippione, D. Boschi, V. Gaidano, P. Circosta, A. Cignetti, F. Dosio, M.L. Lolli, DHODH Inhibitors and Leukemia: an Emergent Interest for New Myeloid Differentiation Agents Drugs Future, 2018, in press.
[13] A.C. Pippione, A. Federico, A. Ducime, S. Sainas, D. Boschi, A. Barge, E. Lupino, M. Piccinini, M. Kubbutat, J.-M. Contreras, C. Morice, S. Al-Karadaghi, M.L. Lolli, 4-Hydroxy-N-[3,5-bis(trifluoromethyl)phenyl]-1,2,5-thiadiazole-3-carboxamide: a Novel Inhibitor of the Canonical NF-κB Cascade, MedChemComm 8 (2017) 1850–1855.

[14] A.C. Pippione, A. Giraudo, D. Bonanni, I.M. Carnovale, E. Marini, C. Cena, A. Costale, D. Zonari, K. Pors, M. Sadiq, D. Boschi, S. Oliaro-Bosso, M.L. Lolli, Hydroxytriazole derivatives as potent and selective aldo-keto reductase 1C3 (AKR1C3) inhibitors discovered by bioisosteric scaffold hopping approach, Eur. J. Med. Chem. 139 (2017) 936–946.
[15] S. Sainas, A.C. Pippione, M. Giorgis, E. Lupino, P. Goyal, C. Ramondetti, B. Buccinna, M. Piccinini, R.C. Braga, C.H. Andrade, M. Andersson, A.C. Moritzer, R. Friemann, S. Mensa, S. Al-Kadaraghi, D. Boschi, M.L. Lolli, Design, synthesis, biological evaluation and X-ray structural studies of potent human dihydroorotate dehydrogenase inhibitors based on hydroxylated azole scaffolds, Eur. J. Med. Chem. 129 (2017) 287–302.
[16] A.C. Pippione, F. Dosio, A. Ducime, A. Federico, K. Martina, S. Sainas, B. Frolund, M. Gooyit, K.D. Janda, D. Boschi, M.L. Lolli, Substituted 4-hydroxy-1,2,3-triazoles: synthesis, characterization and first drug design applications through bioisosteric modulation and scaffold hopping approaches, MedChemComm 6 (2015) 1285–1292.
[17] A.C. Pippione, I.M. Carnovale, D. Bonanni, M. Sini, P. Goyal, E. Marini, K. Pors, S. Adinolfi, D. Zonari, C. Festuccia, W.Y. Wahlgren, R. Friemann, R. Bagnati, D. Boschi, S. Oliaro-Bosso, M.L. Lolli, Potent and selective aldo-keto reductase 1C3 (AKR1C3) inhibitors based on the benzoisoxazole moiety: application of a bioisosteric scaffold hopping approach to flufenamic acid, Eur. J. Med. Chem. 150 (2018) 930–945.
[18] A. Giraudo, J. Krall, B. Nielsen, T.E. Sorensen, K.T. Kongstad, B. Rolando, D. Boschi, B. Frolund, M.L. Lolli, 4-Hydroxy-1,2,3-triazole moiety as bioisostere of the carboxylic acid function: a novel scaffold to probe the orthosteric gamma-aminobutyric acid receptor binding site, Eur. J. Med. Chem. 158 (2018) 311–321.
[19] M.L. Lolli, M. Giorgis, P. Tosco, A. Foti, R. Fruttero, A. Gasco, New inhibitors of dihydroorotate dehydrogenase (DHODH) based on the 4-hydroxy-1,2,5-oxadiazol-3-yl (hydroxyfurazanyl) scaffold, Eur. J. Med. Chem. 49 (2012) 102–109.
[20] S. Sainas, A.C. Pippione, E. Lupino, M. Giorgis, P. Circosta, V. Gaidano, P. Goyal, D. Bonanni, B. Rolando, A. Cignetti, A. Ducime, M. Andersson, M. Jarva, R. Friemann, M. Piccinini, C. Ramondetti, B. Buccinna, S. Al-Karadaghi, D. Boschi, G. Saglio, M.L. Lolli, Targeting myeloid differentiation using potent 2-hydroxypyrazolo[1,5- a]pyridine scaffold-based human dihydroorotate dehydrogenase inhibitors, J. Med. Chem. 61 (2018) 6034–6055.
[21] I. Fritzson, P.T.P. Bedingfield, A.P. Sundin, G. McConkey, U.J. Nilsson, N-Substituted salicylamides as selective malaria parasite dihydroorotate dehydrogenase inhibitors, Medchemcomm 2 (2011) 895–898.
[22] S. Sainas, A.C. Pippione, A. Giraudo, K. Martina, F. Bosca, B. Rolando, A. Barge, A. Ducime, A. Federico, J.S. Grossert, R.L. White, D. Boschi, M.L. Lolli, Regioselective N alkylation of ethyl 4-Benzyloxy-1,2,3-triazolecarboxylate: a useful tool for the synthesis of carboxylic acid bioisosteres, J. Heterocycl. Chem. (2018), In press.
[23] M. Lolli, S. Narramore, C.W. Fishwick, K. Pors, Refining the chemical toolbox to be fit for educational and practical purpose for drug discovery in the 21st Century, Drug Discov. Today 20 (2015) 1018–1026.
[24] A.C. Pippione, S. Sainas, A. Federico, E. Lupino, M. Piccinini, M. Kubbutat, J.-M. Contreras, C. Morice, A. Barge, A. Ducime, D. Boschi, S. Al-Karadaghi, M.L. Lolli, N-Acetyl-3-aminopyrazoles block the non-canonical NF-kB cascade by selectively inhibiting NIK, MedChemComm 9 (2018) 963–968.
[25] S. Sainas, F. Dosio, D. Boschi, M.L. Lolli, Targeting human onchocerciasis: recent advances beyond ivermectin, In: Annual Reports in Medicinal Chemistry, 2018, pp. 1–38.
[26] M.L. Lolli, C. Giordano, D.S. Pickering, B. Rolando, K.B. Hansen, A. Foti, A. Contreras-Sanz, A. Amir, R. Fruttero, A. Gasco, B. Nielsen, T.N. Johansen, 4-hydroxy-1,2,5-oxadiazol-3-yl moiety as bioisoster of the carboxy function. Synthesis, ionization constants, and molecular pharmacological characterization at ionotropic glutamate receptors of compounds related to glutamate and its homologues, J. Med. Chem. 53 (2010) 4110–4118.
[27] R. Ohno, M. Nagaoka, K. Hirai, A. Uchida, S. Kochi, O. Yamada, J. Tokumura, Synthesis and insecticidal activity of novel 1-alkyl-3-sulfonyloxypyrazole-4-carboxamide derivatives, J. Pestic. Sci. 35 (2010) 15–22.
[28] V.I. Minkin, A.D. Garnovskii, J. Elguero, A.R. Katritzky, O.V. Denisko, The tautomerism of heterocycles: five-membered rings with two or more heteroatoms, in: A.R. Katritzky (Ed.), Advances in Heterocyclic Chemistry, Academic Press, 2000, pp. 157–323.
[29] K.L. Kees, J.J. Fitzgerald Jr., K.E. Steiner, J.F. Mattes, B. Mihan, T. Tosi, D. Mondoro, M.L. McCaleb, New potent antihyperglycemic agents in db/db mice: synthesis and structure-activity relationship studies of (4-substituted benzyl) (trifluoromethyl)pyrazoles and -pyrazolones, J. Med. Chem. 39 (1996) 3920–3928.
[30] M.T. Rahman, H. Nishino, Manganese(III)-based oxidation of 1,2-disubstituted pyrazolidine-3, 5-diones in the presence of alkenes, Tetrahedron 59 (2003) 8383–8392.
[31] S. Guillou, Y.L. Janin, 5-Iodo-3-ethoxypyrazoles: an entry point to new chemical entities, Chemistry 16 (2010) 4669–4677.
[32] M.A. Phillips, R. Gujjar, N.A. Malmquist, J. White, M.F. El, J. Baldwin, P.K. Rathod, Triazolopyrimidine-based dihydroorotate dehydrogenase inhibitors with potent and selective activity against the malaria parasite Plasmodium falciparum, J. Med. Chem. 51 (2008) 3649–3653.
[33] E. Pavadai, K. Chibale, M.F. El, M.A. Phillips, S. Wittlin, S. Wittlin, K.C. de, Identification of new human malaria parasite plasmodium falciparum dihydroorotate dehydrogenase inhibitors by pharmacophore and structure-based virtual screening, J. Chem. Inf. Model. 56 (2016) 548–562.
[34] X. Deng, R. Gujjar, F. El Mazouni, W. Kaminsky, N.A. Malmquist, E.J. Goldsmith, P.K. Rathod, M.A. Phillips, Structural plasticity of malaria dihydroorotate dehydrogenase allows selective binding of diverse chemical scaffolds, J. Biol. Chem. 284 (2009) 26999–27009.
[35] D.E. Hurt, J. Widom, J. Clardy, Structure of Plasmodium falciparum dihydroorotate dehydrogenase with a bound inhibitor, Acta Crystallogr. D Biol Crystallogr. 62 (2006) 312–323.
[36] E.F. Pettersen, T.D. Goddard, C.C. Huang, G.S. Couch, D.M. Greenblatt, E.C. Meng, T.E. Ferrin, UCSF Chimera--a visualization system for exploratory research and analysis, J. Comput. Chem. 25 (2004) 1605–1612.
[37] L.M. Weinstock, P. Davis, B. Handelsman, R.J. Tull, General synthetic system for 1,2,5-thiadiazoles, J. Org. Chem. 32 (1967) 2823–2829.
[38] A.N. Boa, S.P. Canavan, P.R. Hirst, C. Ramsey, A.M. Stead, G.A. McConkey, Synthesis of brequinar analogue inhibitors of malaria parasite dihydroorotate dehydrogenase, Bioorg. Med. Chem. 13 (2005) 1945–1967.
[39] E.A. Neidhardt, S.R. Punreddy, J.E. McLean, L. Hedstrom, T.H. Grossman, Expression and characterization of E. coli-produced soluble, functional human dihydroorotate dehydrogenase: a potential target for immunosuppression, J. Mol. Microbiol. Biotechnol. 1 (1999) 183–188.
[40] P. Savitsky, J. Bray, C.D. Cooper, B.D. Marsden, P. Mahajan, N.A. Burgess-Brown, O. Gileadi, High-throughput production of human proteins for crystallization: the SGC experience, J. Struct. Biol. 172 (2010) 3–13.